PB89-169841

Humidification of Flue Gas to Augment SO2 Capture by Dry Sorbents

Southern Research Inst., Birmingham, AL

Prepared for

Environmental Protection Agency
Research Triangle Park, NC

Mar 89

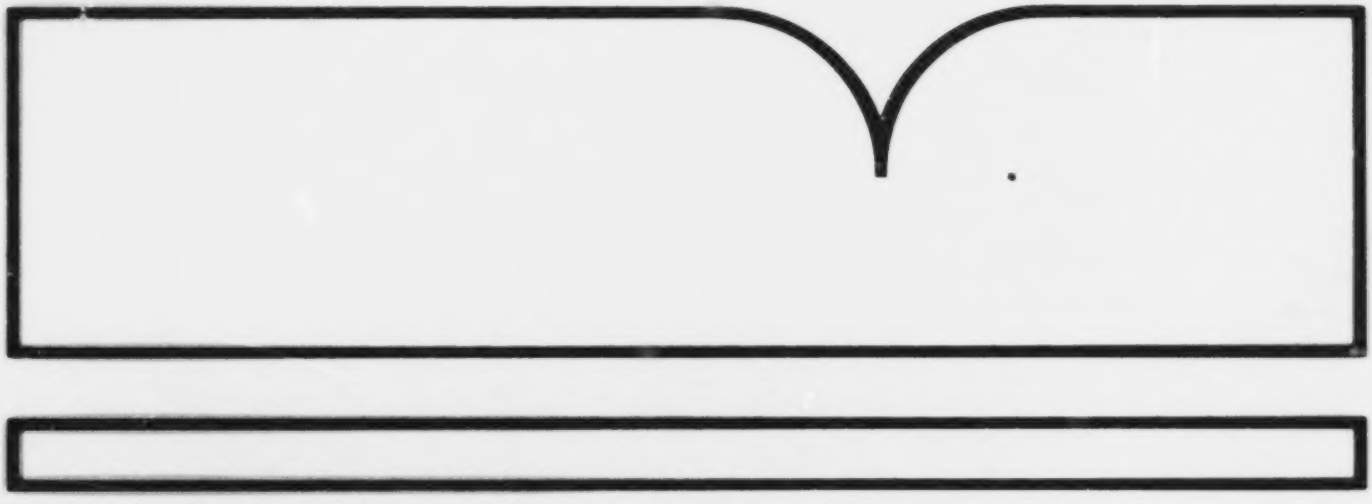

U.S. Department of Commerce
National Technical Information Service
NTIS

TECHNICAL REPORT DATA
(Please read Instructions on the reverse before completing)

1. REPORT NO. EPA-600/7-89-001	2.
3. RECIPIENT'S ACCESSION NO. PB89 169841/AS	
4. TITLE AND SUBTITLE Humidification of Flue Gas to Augment SO_2 Capture by Dry Sorbents	5. REPORT DATE March 1989
	6. PERFORMING ORGANIZATION CODE
7. AUTHOR(S) John P. Gooch, Roderick Beittel, Edward B. Dismukes, and Robert S. Dahlin	8. PERFORMING ORGANIZATION REPORT NO. SRI-ENV-88-1023-5914
9. PERFORMING ORGANIZATION NAME AND ADDRESS Southern Research Institute 2000 Ninth Avenue, South Birmingham, Alabama 35255	10. PROGRAM ELEMENT NO.
	11. CONTRACT/GRANT NO. CR811683 and CR812811
12. SPONSORING AGENCY NAME AND ADDRESS EPA, Office of Research and Development Air and Energy Engineering Research Laboratory Research Triangle Park, NC 27711	13. TYPE OF REPORT AND PERIOD COVERED Final; 10/85-7/88
	14. SPONSORING AGENCY CODE EPA/600/13

15. SUPPLEMENTARY NOTES AEERL project officer is Louis S. Hovis, Mail Drop 4, 919/541-3374. Initially, the project officer was Samuel L. Rakes.

16. ABSTRACT

The report discusses, for a coal-burning power plant, using humidification of the flue gas in a low-temperature duct to increase SO2 removal by dry calcium-based sorbents. In particular, humidification may be a desirable modification of EPA's LIMB process, which is based on injecting limestone or hydrated lime in the furnace; it could augment SO2 removal by adding post-furnace removal to that occurring in the injection zone. This report covers work in post-furnace humidification, charge-augmented humidification, water vapor adsorption by lime (with and without additives), and mathematical modeling of humidification and SO2 removal processes. From these investigations, it was concluded that, for enhancement of SO2 capture at the Edgewater demonstration of LIMB, humidification by a water spray will be required. A spray of pure water would suffice if the frequency of collisions between sorbent particles and water droplets could be increased. Otherwise, isolation of partially sulfated sorbent followed by rehydration and reinjection in a spray will be necessary. Charge-augmented sorbent humidification appears unlikely to enhance sorbent reaction with SO2 under post-furnace conditions. Deliquescent additives that are known to enhance SO2 capture by Ca(OH)2 at low temperatures must operate to some extent by mechanisms other than deliquescence.

17. KEY WORDS AND DOCUMENT ANALYSIS

a. DESCRIPTORS	b. IDENTIFIERS/OPEN ENDED TERMS	c. COSATI Field/Group
Pollution Flue Gases Humidification Sulfur Dioxide Sorbents Calcium Coal Combustion Mathematical Models	Pollution Control Stationary Sources	13B 21D 21B 13H, 13A 12A 07B 11G

18. DISTRIBUTION STATEMENT Release to Public	19. SECURITY CLASS (This Report) Unclassified	21. NO. OF PAGES 76
	20. SECURITY CLASS (This page) Unclassified	22. PRICE

EPA Form 2220-1 (9-73)

PB89-169841

EPA-600/7-89-001
March 1989

HUMIDIFICATION OF FLUE GAS TO AUGMENT SO_2 CAPTURE BY DRY SORBENTS

by
John P. Gooch
Roderick Beittel
Edward B. Dismukes
Robert S. Dahlin
Southern Research Institute
Birmingham, Alabama 35255

EPA Cooperative Agreements No. CR 811683
and No. CR 812811

EPA Project Officer
Louis S. Hovis
Air and Energy Engineering Research Laboratory
U.S. Environmental Protection Agency
Research Triangle Park, North Carolina 27711

AIR AND ENERGY ENGINEERING RESEARCH LABORATORY
OFFICE OF RESEARCH AND DEVELOPMENT
U.S. ENVIRONMENTAL PROTECTION AGENCY
RESEARCH TRIANGLE PARK, NC 27711

REPRODUCED BY
U.S. DEPARTMENT OF COMMERCE
NATIONAL TECHNICAL INFORMATION SERVICE
SPRINGFIELD, VA. 22161

ABSTRACT

In a coal-burning power plant, humidification of the flue gas in a low-temperature duct is a possible way to increase SO_2 removal by dry calcium-based sorbents. In particular, humidification may be a desirable modification of EPA's LIMB process, which is based on the injection of limestone or hydrated lime in the furnace; it could augment SO_2 removal by adding post-furnace removal to that occurring in the injection zone. Southern Research has investigated certain aspects of low-temperature SO_2 removal in humidified flue gas. This report covers work in post-furnace humidification, charge-augmented humidification, water vapor adsorption by lime with and without additives, and mathematical modeling of humidification and SO_2 removal processes. From these investigations, it was concluded that for enhancement of SO_2 capture at the Edgewater demonstration of LIMB is concerned, humidification by a water spray will be required. A spray of pure water would suffice if the frequency of collisions between sorbent particles and water droplets could somehow be increased. Otherwise, isolation of partially sulfated sorbent followed by rehydration and reinjection in a spray will be necessary. Charge-augmented sorbent humidification appears unlikely to enhance sorbent reaction with SO_2 under post-furnace conditions. Deliquescent additives that are known to enhance SO_2 capture by $Ca(OH)_2$ under low-temperature conditions clearly must operate to some extent by mechanisms other than deliquescence per se. The mathematical model gives an improved appreciation of factors that are critical to SO_2 capture by $Ca(OH)_2$ when the sorbent particles are subject to wetting.

NOTICE

This document has been reviewed in accordance with U.S. Environmental Protection Agency policy and approved for publication. Mention of trade names or commercial products does not constitute endorsement or recommendation for use.

CONTENTS

	Page
Abstract	ii
Figures	iv
Tables	vi
Acknowledgments	vi
1. Introduction	1-1
2. Conclusions	2-1
3. Pilot-Scale Investigation of Post-Furnace Humidification to Achieve Sorbent Activation	3-1
Introduction	3-1
Experimental Apparatus	3-1
Humidification of Reinjected Calcine	3-5
Humidification of Hydrated Lime	3-7
Humidification of Entrained Calcine	3-11
Effects of Wall Deposits	3-11
Conclusions	3-13
4. Pilot-Scale Investigation of Charge-Augmented Sorbent Humidification (CASH)	4-1
Introduction	4-1
Preliminary Studies (Cooperative Agreement CR 811683)	4-1
Continued Studies (Cooperative Agreement CR 812811)	4-6
Conclusions	4-18
5. Laboratory Studies of Water-Vapor Adsorption by $Ca(OH)_2$ With and Without Additives	5-1
Introduction	5-1
Background	5-1
Experimental Methods	5-6
Experimental Results	5-9
Conclusions	5-17
6. Mathematical Modeling of Humidification and SO_2 Removal Processes	6-1
Introduction	6-1
Sorbent Wetting and Activation	6-1
SO_2 Capture	6-2
Limiting Assumptions	6-4
Modeling Results	6-4
Conclusions	6-7
7. References	7-1
Appendix: Quality Control Evaluation Report	A-1

FIGURES

Number		Page
3-1	Humidification chamber showing injection and sampling points.	3-3
3-2	Schematic representation of humidification modes.	3-5
3-3	Solids utilization and ΔSO_2 versus time for reinjection of partially sulfated calcine into flue gas with precooling.	3-8
3-4	Solids utilization and ΔSO_2 versus time for reinjection of partially sulfated calcine followed by humidification with a water spray.	3-9
3-5	Solids utilization and ΔSO_2 versus time for injection of partially sulfated calcine in slurry.	3-10
3-6	Composition of samples taken from inlet and outlet of humidifier. Gas firing with 70° burner swirl, furnace injection of hydrated lime, humidification with ST47. Continuous sorbent addition.	3-12
4-1	Spray chamber and residence time chamber.	4-2
4-2	Disc-type ionizer.	4-4
4-3	Apparatus for drop charging and charge measurement.	4-4
4-4	Charge augmentation of humidification to enhance SO_2 capture with limestone injection.	4-5
4-5	Position of ionizer and water nozzle in the pilot combustor.	4-7
4-6	V-I curve for disc ionizer. Firing gas at 1.0×10^6 Btu/hr (300 kW). Injecting SO_2 to burner.	4-9
4-7	Ionization chamber and wire ionizer.	4-10
4-8	Wire-pipe V-I curves with natural gas firing.	4-11
4-9	Sonic Development spray nozzle ST47.	4-13
4-10	Effect of water flow rate and nozzle voltage on the average water droplet charge.	4-14
4-11	Trace of SO_2 concentration in pilot furnace during CASH experiments.	4-17

FIGURES (continued)

Number		Page
5-1	Water vapor suppression by dissolved NaCl or NaOH at 60 °C.	5-3
5-2	Ranges of deliquescence of various sodium compounds at 60 °C (deliquescence occurs in shaded range of p/p^0).	5-4
5-3	Water vapor adsorption on $Ca(OH)_2$ and $CaCO_3$ as reported by Klingspor et al. (13).	5-5
5-4	Schematic diagram of manifold, gas and sample attachment and pressure measuring system of the Accusorb 2100 analyzer.	5-7
5-5	Adsorption and desorption isotherms for $NaCl/Ca(OH)_2$ system at 60 °C.	5-10
5-6	Adsorption isotherms for $Ca(OH)_2$ with and without additives at 60 °C.	5-12
5-7	Comparison of predicted and observed adsorption relationships of $LiCl/Ca(OH)_2$ and $NaCl/Ca(OH)_2$ systems.	5-15
5-8	Comparison of predicted and observed adsorption relationships of $Na_2CO_3/Ca(OH)_2$ and $CaCl_2/Ca(OH)_2$ systems.	5-16
5-9	Humidities required for deliquescence versus approach to saturation.	5-18
6-1	Effect of approach to saturation on SO_2 removal and evaporation time.	6-5
6-2	Predicted SO_2 removal and droplet MMD as a function of residence time.	6-5
6-3	Effect of initial drop diameter on SO_2 removal and evaporation time.	6-6
A-1	Multipoint calibration of Dupont SO_2 Analyzer	A-4

TABLES

Number		Page
3-1	Tests of Reaction in the Dilution Probe.	3-4
3-2	Composition of Partially Sulfated Calcine for Reinjection Tests.	3-4
4-1	Particle Charge Levels from Wire-Pipe Ionizer.	4-12
4-2	Removal of SO_2 During Experiments with the Disc Ionizer.	4-16
4-3	Removal of SO_2 During Experiments with the Wire-Pipe Ionizer (Coal Firing).	4-16
5-1	Experimental Data on the Uptake of Water Vapor by $Ca(OH)_2$-Containing Systems at 60 °C.	5-11
5-2	Water Activity and Partial Pressure for LiCl Systems Based on Gibbard and Scatchard Data (11).	5-14

ACKNOWLEDGEMENTS

The authors wish to acknowledge the guidance and support of the management and staff of the Engineering Applications Division of EPA's Air and Energy Engineering Research Laboratory. Sam L. Rakes and Louis S. Hovis served as project officers through the term of the investigations described in this report. James H. Abbott, Dennis C. Drehmel, and J. David Mobley provided general guidance and support.

The authors also wish to acknowledge the contributions of the technical staff within the Environmental Sciences Department of Southern Research Institute. The main contributors were Bruce A. Morgan, James L. DuBard, Walter R. Dickson (deceased February 1988), and E. Alexander Stokes, III.

SECTION 1

INTRODUCTION

This is a special report summarizing research at Southern Research Institute on the subject of flue-gas humidification as a means of increasing the efficiency of SO_2 removal by dry sorbents. The research was conducted for the Environmental Protection Agency as part of the overall efforts under two Cooperative Agreements, CR 811683 and CR 812811. The work described here was performed between October 1, 1985, and July 1, 1988.

EPA has been developing the dry-sorbent technology known as LIMB over the past several years as a means of lowering SO_2 emissions from coal-fired power boilers. The acronym stands for Limestone Injection, Multistage Burners. Originally, the process was envisioned as one based on limestone as the specific calcium-based sorbent; currently, however, the process emphasizes the use of hydrated lime — that is, $Ca(OH)_2$ — as a more reactive sorbent in place of limestone. LIMB based on either sorbent, however, depends upon the injection of the sorbent in the furnace at a temperature above 2000 °F (1100 °C), the calcination of the sorbent to CaO, and the reaction of the sorbent with SO_2 in the presence of O_2 to produce $CaSO_4$.

The utilization of the sorbent under these conditions is not high; the utilization does not exceed 25 to 30% on the mole basis and, thus, accounts for removal of only 50 to 60% of the SO_2 present at a practical 2:1 Ca/S mole ratio. Such utilization levels are acceptable for retrofit operations in boilers predating new-source performance regulations. Still, increased utilization is obviously desirable if it can be attained.

Humidification and cooling of the flue gas in a post-furnace duct, beginning at a temperature approximating 300 °F (150 °C), is one conceivable way to enhance the utilization of furnace-injected sorbent. At relatively low temperatures SO_2 can react with the calcine of limestone or hydrated lime to produce $CaSO_3$, whereas at high temperatures in the furnace it reacts only in combination with O_2 to produce $CaSO_4$. The critical issue, however, is not temperature and the thermodynamic possibility of sulfite formation but humidification and the kinetic enhancement of low-temperature reactions, which would be slow without humidification.

Humidification is a means not only of enhancing SO_2 removal with furnace injection of dry sorbents but of achieving SO_2 removal with direct injection of $Ca(OH)_2$ in either the dry or the wet state. Extensive research under the auspices of the Department of Energy has been recently performed and is now continuing on duct-injection processes, which take two basic forms: 1) separate injections of dry $Ca(OH)_2$ and a water spray or 2) simultaneous injection of $Ca(OH)_2$ and water in a slurry. In either process, the sorbent reaches the particulate collector (ESP or baghouse) in a dry state, after the water has evaporated. Maintaining proximity to vapor saturation, however, is the key to effective SO_2 removal.

This report describes four different but related studies of the issue of humidification:

- Section 3. Pilot-scale investigation of post-furnace humidification to achieve sorbent activation. This investigation was carried out with Southern Research's 1 x 10^6-Btu/h (300-kW) coal combustor to support EPA's LIMB demonstration at Ohio Edison's Edgewater power plant at Lorain, Ohio. The central question addressed was what humidification conditions are required for sulfated calcine from the furnace to undergo low-temperature reaction with SO_2. Is humidification by water vapor alone adequate, or is humidification with a water spray required because of the need for physical wetting of the sorbent particles?

- Section 4. Pilot-scale investigation of charge-augmented sorbent humidification (CASH). Once again, the Southern Research pilot-scale combustor was employed to address a question relevant to the Edgewater demonstration. Can opposite electrical charging of sorbent particles and water droplets increase collisions sufficiently to enhance SO_2 removal?

- Section 5. Laboratory studies of water-vapor adsorption by $Ca(OH)_2$ with and without additives. A brief experimental program was conducted to quantify the effects of certain additives on water-vapor uptake by $Ca(OH)_2$. If $Ca(OH)_2$ per se is to be employed in a duct-injection process, use of a deliquescent additive may be desirable. Alternatively, if partially sulfated calcine from furnace-injected sorbent is to be rehydrated outside the power plant and reinjected in a duct process, it may be advantageously treated with a water-attracting additive.

- Section 6. Mathematical modeling of humidification and SO_2 removal processes. A mathematical model was developed to treat two processes: 1) the collision of sorbent particles and water droplets from a spray nozzle and 2) the capture of SO_2 by the wetted sorbent particles. Interaction parameters considered included particle and droplet sizes, relative velocities, proximity to saturation, residence time, and Ca/S ratio.

SECTION 2

CONCLUSIONS

The investigation of the fundamentals of sorbent humidification (Section 3) led to the primary conclusion that humidification by water vapor alone does very little toward enhancing SO_2 removal by partially sulfated calcine, whereas humidification by a water spray has the potential to enhance SO_2 removal substantially, provided that sorbent particles and water droplets collide with reasonable efficiency. The low-temperature pickup of SO_2 by partially sulfated calcine, in which the utilization factor was 18% in the furnace, was tested by three humidification modes. Each mode involved the same temperature and humidity and the same approach to saturation at the steady state existing once all added liquid water had evaporated; each mode also involved reinjection of the calcine in a low-temperature duct. Water vapor alone caused the utilization factor to increase by about 1% (from 18 to 19%); a water spray separate from the solid gave an increase of 6%; finally, a slurry made from the solids and liquid water gave an increase of about 30%. Recycle of unreacted sorbent to increase contact time was outside the scope of these studies.

What is needed, clearly, if furnace-injected calcine is to be activated in situ by humidification, is the introduction of a water spray under conditions that will provide efficient collisions between water droplets and sorbent particles. Inefficient collisions accounted for the low enhancement of SO_2 capture from the separate water spray. Wetting, if it occurs, will obviously release active base from the sorbent particles and give marked enhancement of SO_2 capture, as the results with the slurry demonstrate.

The use of charge-augmented sorbent humidification (Section 4) seemed to offer prospects for increased frequency of sorbent-droplet collisions. The concept of CASH was that negative charging of sorbent particles and positive charging of water droplets would ensure efficient interaction. In none of the studies of CASH performed, however, was any favorable effect on sorbent utilization discerned. The reasons for this disappointing result are not clear-cut. One possible explanation, however, is that the attractive force between oppositively charged sorbent particles and water droplets is small; it decreases with the square of the separating distance and is small in comparison with other electrical forces except when the separating distance is of the order of the particle dimensions. The other electrical forces arise from the lack of precise electrical balance between positive and negative charges, thus creating a net "space charge" field. In the absence of zero as a net charge in the cloud of particles and droplets, an electrical force operates on each, bringing about a separation and deposition on the container walls.

The use of deliquescent additives in a sorbent is another means of overcoming the difficulty of achieving efficient interaction of sorbent particles and water droplet. The concept is that the affinity of the sorbent for water vapor could be so high that the sorbent would be physically wetted irrespective of collisions with water droplets. Characterization of the effects of certain water-attracting additives through the measurement of water-vapor adsorption isotherms (Section 5) has provided insight to the conditions where physical wetting occurs. Some additives seem to behave independently from the $Ca(OH)_2$

medium in which they are placed; examples are LiCl and NaCl, which require highly different levels of relative humidity for deliquescence (LiCl, about 10%; NaCl, about 75%). Other additives interact with $Ca(OH)_2$ and do not behave as they would alone; an example is $CaCl_2$, which is much less deliquescent in the mixture than it is alone. Because of the inconsistencies between measured effects of these additives on water vapor uptake and reported effects on SO_2 removal, one obvious conclusion is that some of the additives function through mechanisms other than inducing physical wetting of the sorbent.

The results of the modeling study (Section 6) show that, when lime and water are injected separately, the SO_2 removal efficiency is governed by the degree of sorbent wetting by collisions between sorbent particles and water droplets. The sorbent/droplet collision rate is maximized by making the droplet size and velocity as large as possible. In actual practice, however, the droplet size must be well below the optimum value in order to assure complete evaporation and avoid wetting of the duct walls. If the humidification process could be modified to allow larger droplets, it would be possible to significantly improve on the sulfur capture achieved.

The sulfur capture is strongly influenced by approach to saturation, Ca/S ratio, and residence time, as well as droplet size and velocity. To maximize SO_2 removal, the approach should be as close as possible. However, it may be difficult to consistently maintain dry duct walls at approaches of less than 20 °F (11 °C). Increasing the sorbent injection rate, or Ca/S ratio, is also beneficial, but reaches a point of diminishing returns due to increased operating cost and particulate loadings. The effect of the latter on ESP performance must also be considered.

Increasing the residence time is only beneficial up to the point of complete droplet evaporation. Conversely, the residence time must be at least sufficient to allow complete evaporation. For most retrofit situations, the residence time will be fixed. This means that the droplet size must be selected to make maximum use of the available time without allowing droplets to reach the ESP. The model can be used to predict the optimum droplet sizing for a given duct residence time.

SECTION 3

PILOT-SCALE INVESTIGATION OF POST-FURNACE HUMIDIFICATION TO ACHIEVE SORBENT ACTIVATION

INTRODUCTION

Post-furnace humidification is receiving a great deal attention currently as a means of enhancing the reaction of dry calcium-based sorbents with SO_2 at relatively low gas temperatures in ducts approaching the stack. In some instances, this technique is intended to increase the utilization of sorbents that are injected into the furnace to undergo primary reaction at high temperatures; for example, Yoon et al. of Consol R & D (1) have described a process called "BLI Activation," in which limestone is injected in the boiler and the resulting calcine is activated by humidification in a low-temperature duct to undergo further reaction with SO_2. In other instances, the sorbent is only injected in the low-temperature duct; it undergoes all of its reaction in this zone and is highly dependent upon humidification to achieve significant reaction. One example of the low-temperature process has been referred to by Yoon et al. as "Straight Coolside;" it is based on $Ca(OH)_2$ as the sorbent and humidification with a spray of liquid water, which evaporates to further lower the reaction temperature. Low-temperature or duct-injection processes have been investigated under EPA- and EPRI-sponsored programs (2,3) and are currently under intensive development by the Department of Energy as a means for reducing the problem of acid rain.

One of the crucial issues associated with post-furnace humidification is whether activation can be achieved with water vapor alone or can only be accomplished by physical contact between sorbent particles and liquid water droplets prior to their evaporation. Another issue is how the effect of liquid droplets can be optimized by controlling droplet size, residence time, and other parameters. In ultimate efficiency, the interaction of sorbent particles and water droplets may approach that in a spray dryer. Comparison of vapor humidification and spray humidification with spray drying, therefore, is an appropriate way to gauge the effectiveness of the two humidification processes.

Post-furnace humidification has been viewed as a possible means of increasing the utilization of $Ca(OH)_2$ sorbent in the Edgewater demonstration. Humidification will be depended upon to satisfy one other essential goal — adjustment of the ash-sorbent electrical resistivity to a lower value consistent with efficient electrostatic precipitation. Obviously, the process will be even more useful if it improves SO_2 removal. Post-humidification at Edgewater would be a process parallel to Consol R & D's "BLI Activation" process; it would differ, however, in that the sorbent at Edgewater is hydrated lime, whereas that in Consol R & D's process is limestone.

EXPERIMENTAL APPARATUS

The main component of the experimental apparatus used for the post-furnace humidification studies was a cylindrical humidification chamber on a vertical

axis, which is illustrated in Figure 3-1. This chamber was inserted between segments of the 4-in. (10-cm) duct normally channeling flue gas at a temperature around 300 °F (150 °C) to the system exit. The inlet and outlet of the chamber were flared outward to a diameter of 36 in. (91 cm); the length of the chamber was about 10 ft (3 m). Thermocouples were mounted at intervals along the length of the chamber. A Sonic Development (ST47) two-fluid nozzle was placed at the centerline near the inlet for injecting water or an aqueous slurry. The total residence time of flue gas in the chamber was 10 to 15 s, much longer than the time that would exist in an actual power-plant duct. The geometry, however, minimized collision of water droplets with the walls; moreover, the chief objective was to determine the upper limit of reaction. When water droplets were injected, their short lifetime (about 1 s) rather than the total gas residence time was the controlling factor on the extent of reaction.

The nozzle was operated at an air pressure of 80 psi (550 kPa) and a water flow rate of 5.75 mL/s. Sizing of the spray droplets with Southern Research's Video Droplet Analyzer indicated that the mass-median diameter was about 35 μm. The estimated time required for the droplets to undergo complete evaporation under the experimental conditions subsequently described was about 1.2 s. The ST47 nozzle was also used for slurry injection on occasion, as a substitute for water injection. Dry solids, on the other hand, were injected in a stream of air at a location immediately upstream from the humidification chamber.

A dilution probe was used to sample entrained solids at the outlet of the reactor. This probe dilutes the sample with hot, dry air through a porous wall just inside the inlet and performs the vital function of quenching reaction at the instant of sampling. A filter was used to collect solids from flue gas sampled at about 0.003 ft^3/s (0.1 L/s) and a dilution of 10:1. Analysis of these solids provided the data that were used to compute the utilization of the sorbent. This procedure was eminently superior to the use of results based on the change in gas-phase SO_2 concentration, which was heavily influenced by reaction with long-lived wall deposits.

Details of a validation test of the dilution probe are given in Table 3-1. Hydrated lime was injected just upstream of the humidification chamber and followed by humidification to a total water concentration of 0.24 mole of water per mole of dry flue gas from an initial value of 0.17 mole/mole. The dilution probe was used to sample SO_2-free flue gas (from the combustion of natural gas) at the chamber outlet where the approach to saturation varied from 20 to 40 °F (11 to 22 °C) from experiment to experiment. The dilution air was spiked with SO_2 — 2000 ppm; the dilution air volume was about four times the sample volume. Under these extreme conditions, the in-probe conversion of $Ca(OH)_2$ was about 2% or less.

An alternate sampling system — isokinetic with an in-duct filter — was used to determine the concentration of total suspended solids at the chamber outlet. It was also used on occasion at the inlet. There was no requirement at the outlet for the system to prevent further chemical reaction during sampling. On the other hand, the system was required to prevent reaction when used at the inlet (when sorbent was injected upstream from the inlet, prior to injection of water); the system was found satisfactory with respect to this requirement.

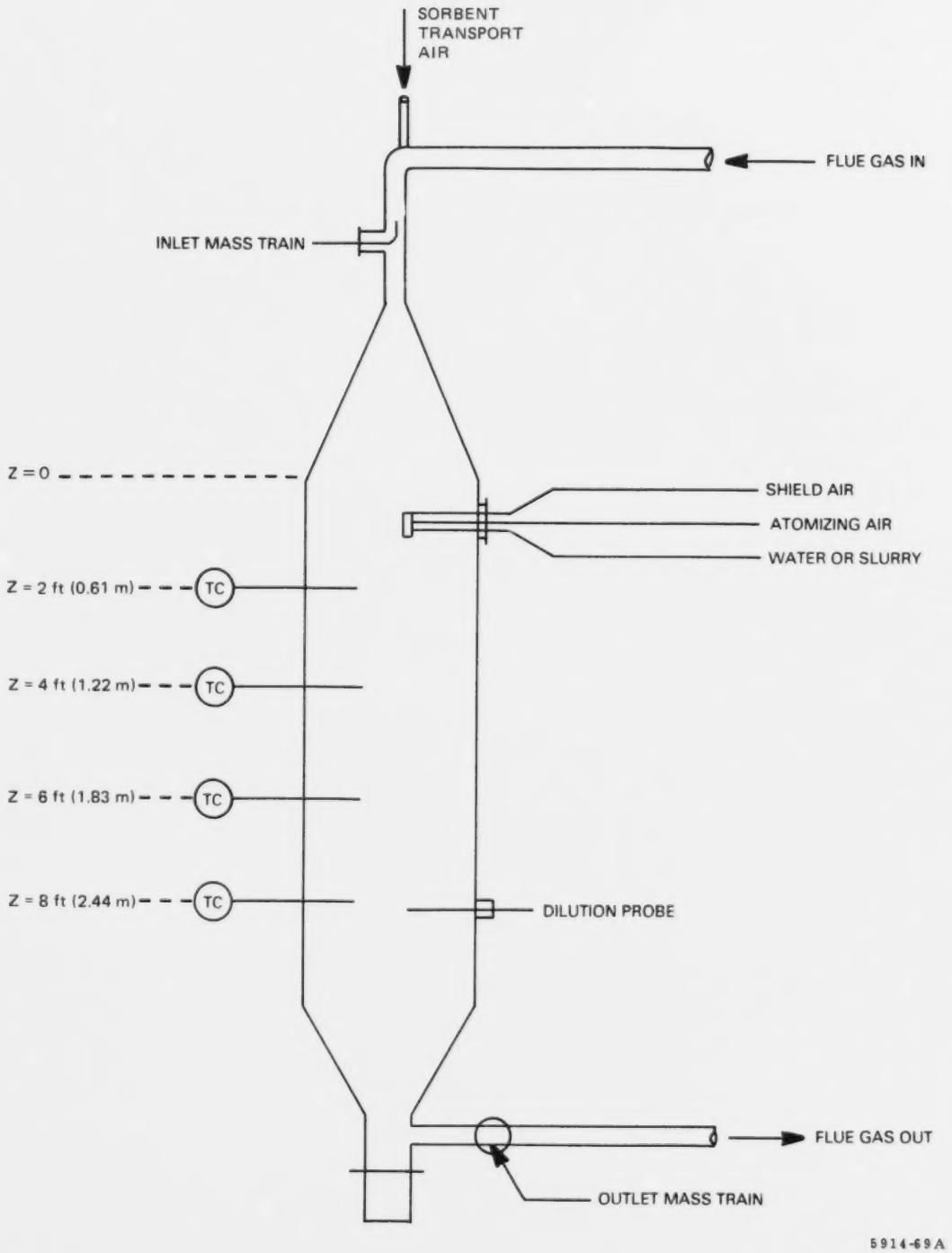

Figure 3-1. Humidification chamber showing injection and sampling points.

Table 3-1. Tests of Reaction in the Dilution Probe[a]

Expt	S/Ca		
	Dilution probe	Mass train	Difference[b]
1	0.058	0.041	0.017
2	0.033	0.014	0.019
3	0.032	0.011	0.021
4	0.028	0.012	0.016

a. Dry $Ca(OH)_2$ injected at the chamber inlet, followed by humidification to a 20-40 °F (11-22 °C) approach. Simultaneous samples at the humidifier outlet with the dilution probe and mass train. SO_2 was present only in the dilution air. Dilution probe operated with 7 L/min flue gas diluted 4:1 with dry air at 300 °F (150 °C) containing 2000 ppm SO_2. Twenty-minute run time, sample collected in a filter.

b. Since no SO_2 was present in the flue gas, the mass train S/Ca is a measure of reentrained, sulfated material, which had been deposited on the duct walls during earlier experiments. The extent of reaction in the dilution probe is therefore the difference in S/Ca between the two samples.

Table 3-2. Composition of Partially Sulfated Calcine for Reinjection Tests

Component	Weight %	fraction of mole total Ca
CaO	33	0.49
$Ca(OH)_2$	23	0.26
$CaCO_3$	7	0.06
$CaSO_4$	30	0.18
Other	7	-

HUMIDIFICATION OF REINJECTED CALCINE

To facilitate a systematic study of humidification parameters, a large quantity of partially sulfated calcine was prepared for reinjection into the flue-gas stream immediately upstream from the humidification chamber. Reinjection of this material, followed by humidification, gave a simulation of the processes to be expected at the Edgewater demonstration if post-furnace humidification were to be adopted. The material was produced by injecting $Ca(OH)_2$ into the furnace at a Ca/S ratio of 2 during the addition of SO_2 to the combustion products from natural gas. The material was collected on the fabric filter at the exit from the combustor. Chemical analysis showed that the composition of material on the weight basis was 33% CaO, 23% $Ca(OH)_2$, 7% $CaCO_3$, 30% $CaSO_4$, and 7% other components. The calculated atom ratio Ca/S in the solid corresponded to a utilization of 18% in the furnace. Full details of the composition are given in Table 3-2.

The reinjected calcine was subjected to the effects of humidification by three processes, as depicted schematically in Figure 3-2. First, the dry solid was injected into flue gas containing excess water vapor, which had been precooled to 160 °F (71 °C). At no time during this process was liquid water introduced, and thus at no time did the calcine become physically wet. Literally speaking, there was no humidification in this process, but the effects

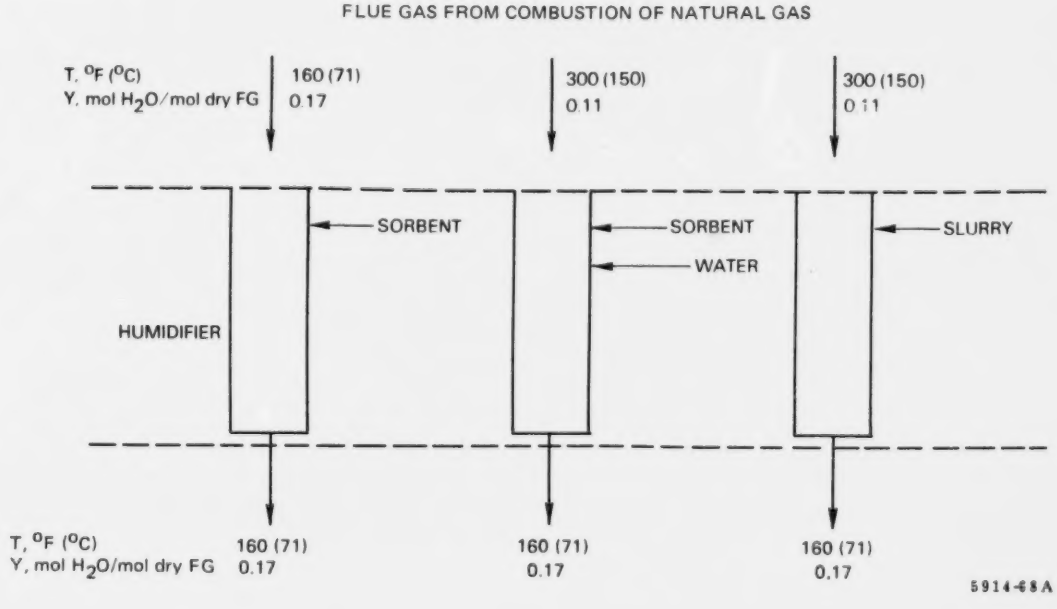

Figure 3-2. Schematic representation of humidification modes.

simulated humidification by vapor addition and convective cooling, with heat discharged to the surroundings. Second, the dry solid was injected into flue gas at a temperature near 300 °F (150 °C) and then liquid water was introduced as a spray to cool the flue gas to 160 °F (71 °C). Third, the solid was briefly slurried with water and then introduced as a spray at 300 °F (150 °C), which subsequently lowered the gas temperature to 160 °F (71 °C). (To facilitate spraying the slurry, a small impingement target near the exit of the ST47 nozzle, known as the resonator, was removed; the resonator was usually retained for spraying plain water.) The features common to all three processes were these: 1) the flue gas was generated by the combustion of natural gas; 2) the SO_2 was added from an external source to a concentration of 1100 ppm; 3) reaction of SO_2 with the solids occurred at the same temperature, the same humidity level, and the same approach to adiabatic saturation. The temperature was 160 °F (71 °C), which represented a 30 °F (17 °C) approach to saturation; the water vapor concentration was 0.17 mole of water per mole of dry flue gas. One of the primary differences in conditions was in the O_2 level; to make it possible to humidify the combustion gas from natural gas to the final level desired, the gas was burned with excess air when liquid water or slurry was to be injected. Another difference was in the Ca/S ratio in the humidification chamber; the ratio was 2 in the first and second methods but only 1 in the third, with slurry injection.

Determinations of sorbent utilization following humidification revealed increments in utilizations over the 18% absolute level that had occurred previously in the furnace as follows:

Humidification method	Increment in utilization
Cooling to enhance the effect of water vapor already present	1%
Cooling and humidification with a water spray	6%
Slurrying with liquid water and spray injection	33%

Very little reaction of SO_2 with the calcine occurred when only water vapor was present. A six-fold increase in reaction, giving an increment in utilization of 6%, occurred when the dry solid was subjected to the effects of a water spray. An increment in excess of 30% occurred with slurry injection. Comparison of the results obtained with the water spray and the slurry spray indicates that the extent of low-temperature reaction was controlled by the fraction of sorbent particles actually colliding with water droplets and becoming physically wet. The added increment due to the water spray (5%) divided by the increment due to the slurry spray (33%) is indicative of a collision efficiency of 15% (5/33 x 100 = 15).

The slurry was prepared on-line in order to minimize the time available for reaction of the water and calcine. Slaking tests with quicklime and sulfated calcine have shown that the latter material hydrates much more slowly, presumably due to the presence of a $CaSO_4$ layer. An initial concern was that this effect might prevent the activation of a sorbent particle in the time available in a humidifier. Although the estimated sorbent-water contact time of 30-60 s was much longer than that available in an evaporating droplet, the results show that the rate of hydration is not inhibited to the degree indicated by the slaking tests.

Figure 3-3, 3-4, and 3-5 present data from experiments with the three modes of sorbent injection. In each of the first two figures, the upper graph shows a gradually increasing removal of SO_2 during much of the period of sorbent injection. On the other hand, the lower graph for solid analysis shows reasonably consistent results on increases in sorbent utilization. The latter are the data summarized in the table above; the gas-phase data are indicative of extensive reaction by wall deposits.

HUMIDIFICATION OF HYDRATED LIME

To determine the effects of humidification on a sorbent that had not been subjected to a high-temperature calcination, $Ca(OH)_2$ was injected into the flue-gas duct immediately upstream from the humidifier and allowed to react with SO_2 under the same conditions as those in the experiments with the partially sulfated calcine. The Ca/S mole ratio in each case was 2. The degrees of utilization observed following low-temperature reaction were as follows:

Humidification method	Extent of utilization
Cooling to enhance the effect of water vapor already present	9.6%
Cooling and humidification with a water spray	12%
Slurrying with liquid water and spray injection	28%

The results with the hydrated lime differ from those with the partially sulfated calcine primarily in terms of the effects produced by cooling alone and by the combination of spray humidification and cooling. Cooling alone gave a utilization of nearly 10% with the hydrated lime but an increment of just 1% with the calcine. The presence of water spray, on the other hand, increased the utilization of hydrated lime only from 10 to 12% but increased that of the calcine from 1 to 6%. Slurrying gave about the same result with both sorbents; this was a utilization of about 30% total with the hydrated lime or about 30% incrementally with the calcine.

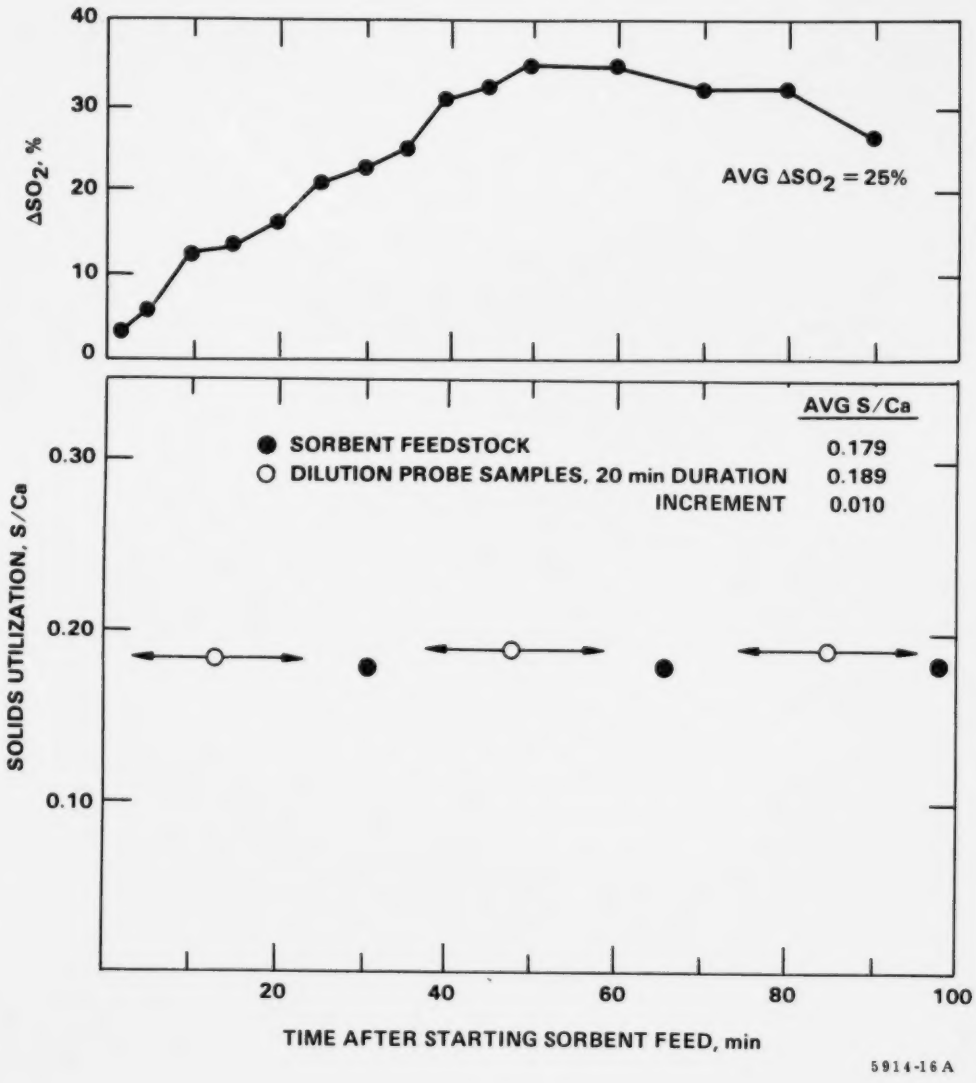

Figure 3-3. Solids utilization and ΔSO_2 versus time for reinjection of partially sulfated calcine into flue gas with precooling.

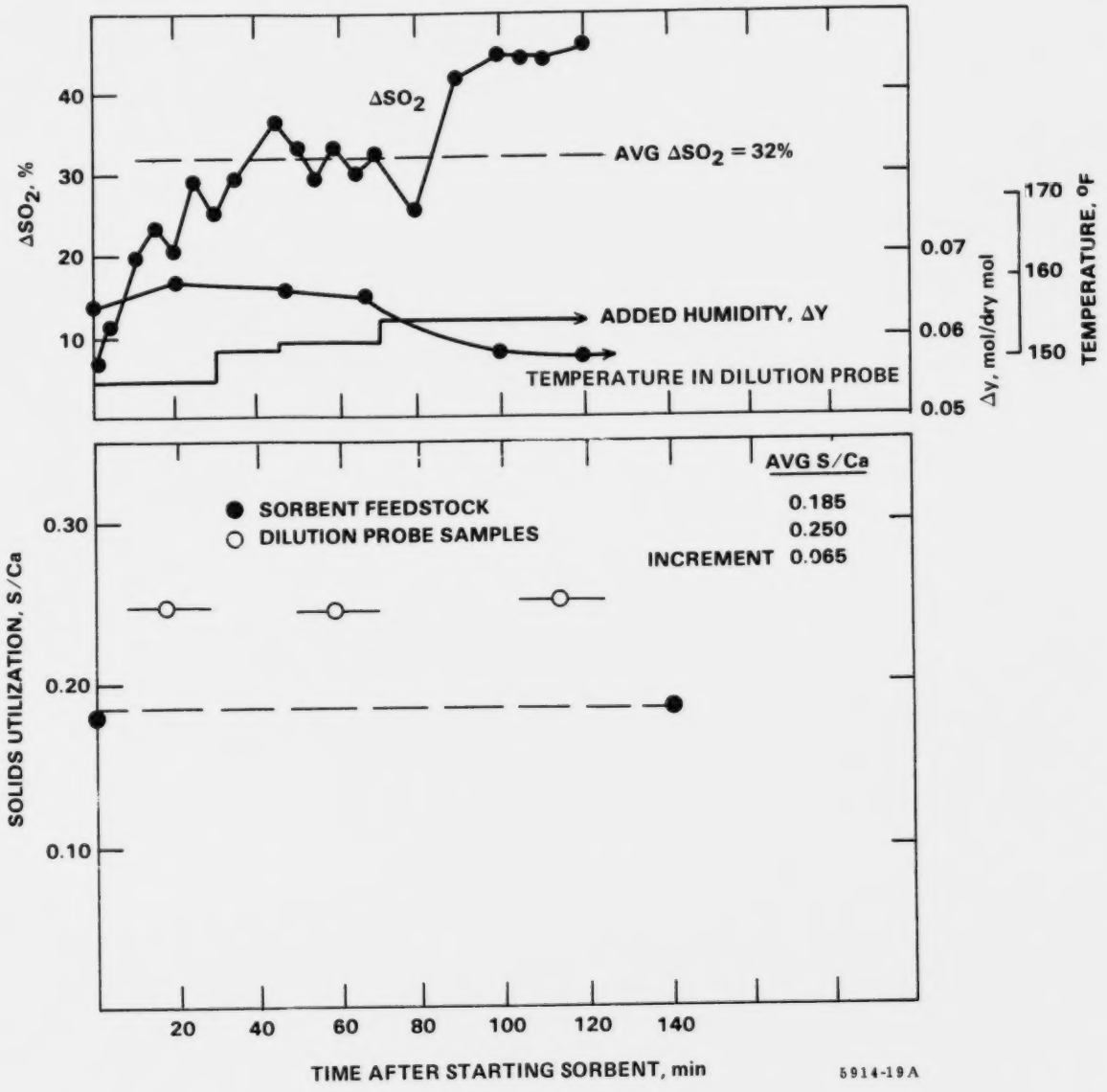

Figure 3-4. Solids utilization and ΔSO_2 versus time for reinjection of partially sulfated calcine followed by humidification with a water spray.

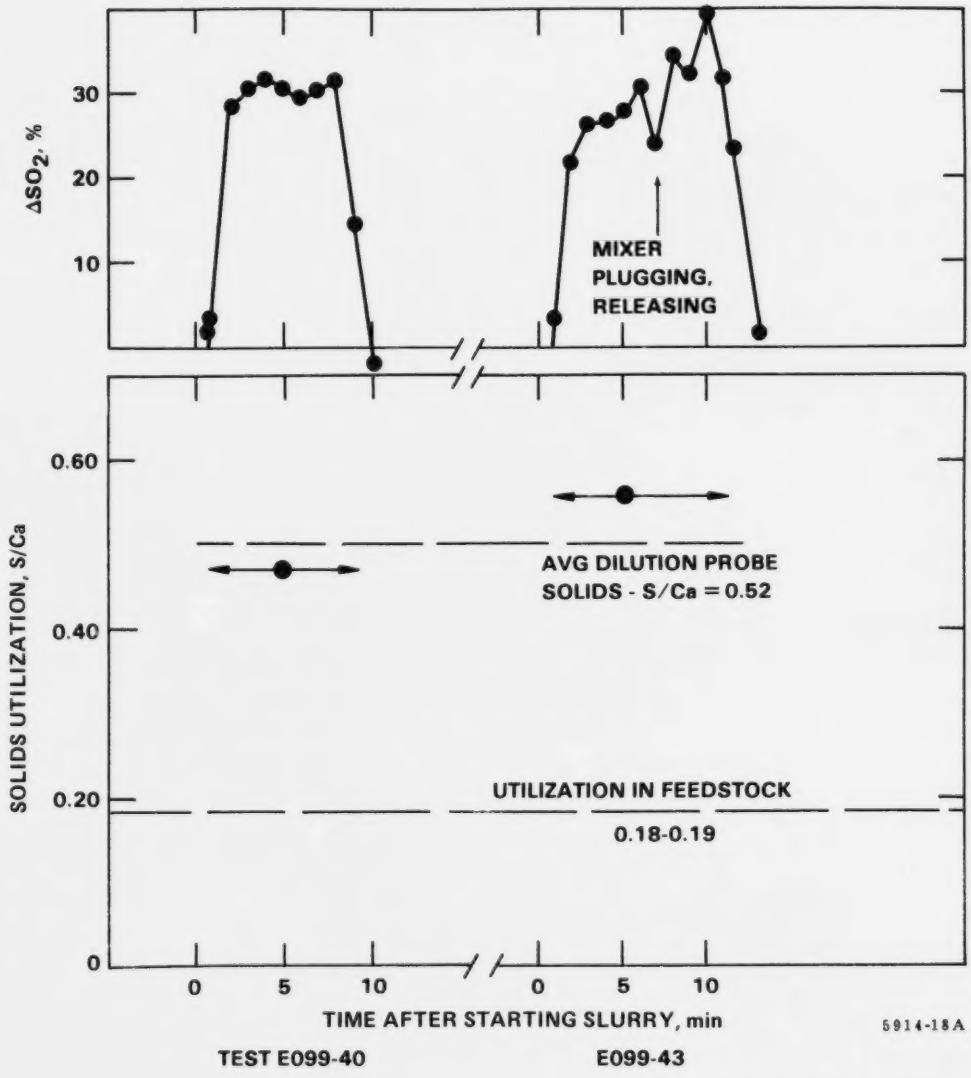

Figure 3-5. Solids utilization and ΔSO_2 versus time for injection of partially sulfated calcine in slurry.

The similar effects of slurrying the calcine and the hydrated lime are particularly striking. They indicate that the shell of $CaSO_4$ product surrounding a core of unused sorbent in the calcine particles is not a strong deterrent to the promotional effects of liquid water. Evidently, the $CaSO_4$ shell sloughs off rapidly when liquid water is present and does not markedly retard the wetting and partial dissolution of the underlying sorbent.

HUMIDIFICATION OF ENTRAINED CALCINE

For a more direct study of the humidification of partially sulfated calcine, $Ca(OH)_2$ was injected in the furnace, was thus subjected to calcination and sulfation in the furnace, and was then humidified at low temperature and subjected to further reaction with SO_2. Again the furnace was gas-fired and doped with SO_2 from an external source; a high level of excess air was used to produce humidity and temperature values at the humidifier that were comparable to those previously investigated. The burner was operated at either of two swirl angles for the secondary air. At 30°, there was a wide range of temperatures at the sorbent injection level — as high as 2780 °F (1525 °C), although the average was only 2070 °F (1130 °C). At 70°, on the other hand, the temperatures were more uniform at the injection level — maximum, 1990 °F (1090 °C); average, 1870 °F (1020 °C).

Utilization levels of the calcine measured at the inlet to the humidification chamber, as the result of sulfation in the furnace, were about 26%. Increments in utilization — due to humidification by the spray injection of liquid water — averaged 3.9% with 30° swirl in the furnace or 1.5% with 70° swirl in the furnace. Data for the latter condition are presented in Figure 3-6. Both increments reported are, of course, substantially lower than that of 6% observed for reinjected calcine with the same humidification method.

Several factors may have contributed to the difference noted above for entrained and reinjected calcine. First, the reinjected calcine was less extensively utilized before humidification (18% rather than 26%). Second, the reinjected calcine was exposed to an SO_2 concentration of about 1100 ppm in the humidifier, whereas the entrained calcine reacted at a lesser concentration of about 700 ppm. Finally, the reinjected calcine was coarser in particle size — a factor that promoted more efficient particle-droplet collisions. It is reasonable to assume that, in general, humidification and cooling with a water spray will promote further reaction to a degree that is governed by the extent of prior reaction in the furnace.

EFFECTS OF WALL DEPOSITS

Data on the utilization of suspended sorbent, based on analyses of solids removed in the dilution probe, usually indicated that the extent of SO_2 reaction was far below that signified by changes in the SO_2 gas-phase concentration. Reaction of SO_2 with the solids deposited on the in-stack filter ahead of the SO_2 analyzer was not a significant contributor to this discrepancy. Hence, reaction of SO_2 with solids deposited on walls within the reaction system was assumed to be the primary cause of the discrepancy.

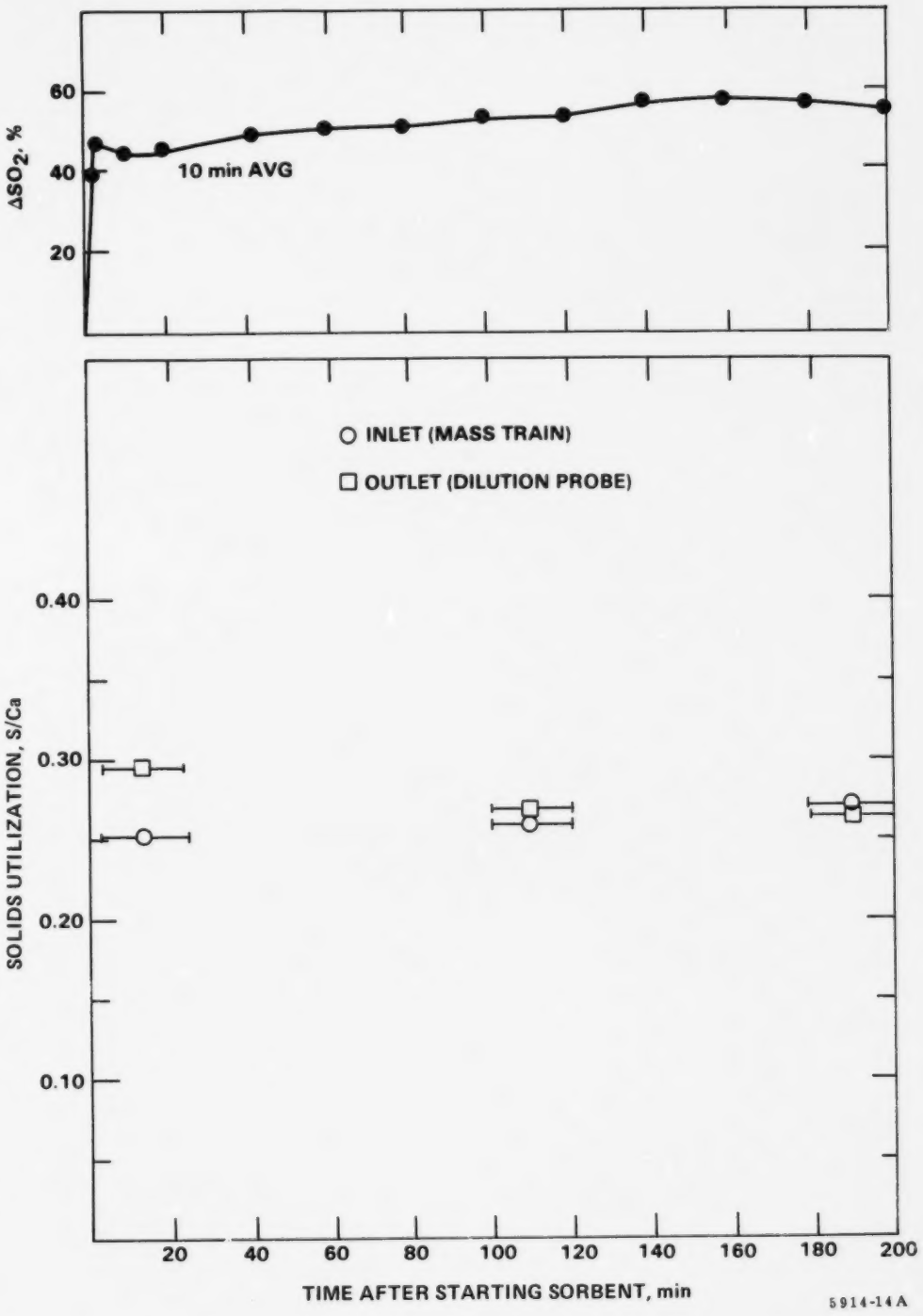

Figure 3-6. Composition of samples taken from inlet and outlet of humidifier. Gas firing with 70° burner swirl, furnace injection of hydrated lime, humidification with ST47 nozzle. Continuous sorbent addition.

To test the validity of this assumption, material balances were attempted during several of the tests described above. Before each test, the humidifier chamber was thoroughly cleaned by brushing and washing. After the test, as much material as possible was removed from different areas of the walls, weighed, and analyzed to determine the amounts of calcium and sulfur in the deposits. During the test, entrained solids were collected in the dilution probe and in a mass train.

The results of material-balance determinations can be illustrated in terms of two experiments. In the first, partially sulfated calcine was injected into humid flue gas (no water was added); in the second, the dry calcine was injected and followed with a water spray. Here is a summary of the results:

- Recovery of calcium — from entrained solids, 32%; from chamber walls, 45%; total, 77%. Recovery of sulfur — from the gas phase, 82%; from entrained solids, 0.5%; from chamber walls, 11.5%; total, 94%. About 64% of the SO_2 removal from the gas phase was found in the wall deposits.

- Recovery of calcium — from entrained solids, 39%; from chamber walls, 47%; total, 86%. Recovery of sulfur — from the gas phase, 60%; from entrained solids, 5%; from chamber walls, 23%; total, 96%. Approximately 72% of the SO_2 removed from the gas phased was found in the wall deposits.

The incompleteness of calcium and sulfur recoveries does not detract from the conclusions reached. Whatever the disposition of unrecovered material may have been, the wall deposits recovered and analyzed still accounted for the fractions of SO_2 loss reported: in the first instance, 11.5/(100 - 82) or 64%; in the second instance, 23/(100 - 68) or 72%.

CONCLUSIONS

Water vapor alone is not effective for activating the removal of SO_2 by partially sulfated calcine at low temperature. Humidification of the sorbent with a water spray is more effective, but even its effectiveness is limited by the infrequency of collisions between the sorbent particles and water droplets. The rapid and extensive rate of reaction of sorbent in a slurry, even after very brief contact between sorbent and water, reveals that the key to successful humidification is increasing the frequency of sorbent-droplet collisions.

SECTION 4

PILOT-SCALE INVESTIGATION OF CHARGE-AUGMENTED SORBENT HUMIDIFICATION (CASH)

INTRODUCTION

The foregoing discussion makes it clear that methods of increasing the frequency of collisions between sorbent particles and water droplets are needed to increase the effectiveness of spray humidification. Modeling studies that have been conducted for EPA under Cooperative Agreement CR 812811 (see Section 6) reveal that the fraction of sorbent particles that can be intercepted by water droplets increases as the droplet size increases, as the droplet velocity increases, and as the sorbent particle size increases. Another concept to be discussed here is that charge augmentation will provide another means for increasing sorbent-droplet interactions. Charge augmentation refers to a process whereby either sorbent particles or water droplets or both are given an electrostatic charge in order to increase their collision rate.

Charge-augmented sorbent humidification, or CASH, is a process conceived jointly by investigators at EPA and Southern Research. The initial work on this process was conducted under Cooperative Agreement CR 811683 and then later continued under another Cooperative Agreement CR 812811.

PRELIMINARY STUDIES (Cooperative Agreement CR 811683)

Experimental Apparatus

The humidification chamber used for the initial CASH experiments is illustrated in Figure 4-1. The chamber was 8 in. (20 cm) in diameter and had a length of about 7 ft (2.1 m). Flue gas entered the chamber from a 4-in. (10-cm) duct at a temperature of about 300 °F (150 °C). Near the point SCI, the gas stream passed an ionizer, which imparted a negative charge to the entrained sorbent particles. Just below the ionizer, at the point SCO, the gas stream passed the spray nozzle, at which positively charged water droplets were injected. In the main part of the humidification chamber, a series of thermocouples were located at positions SC2, SC3, etc.

Beyond the humidification chamber, the flue gas stream passed again through a 4-in. (10-cm) duct and then entered a "residence-time chamber", approximately 12 in. (30 cm) in diameter and 7 ft (2.1 m) in length. The time of residence of the flue gas in this chamber was approximately 1.0 s, compared to a time of about 0.4 s in the humidification chamber. The overall system depicted in Figure 4-1 was in operation before the larger humidification chamber previously illustrated in Figure 3-1 became available; with a higher ratio of surface area to gas volume, the smaller system shown in Figure 4-1 suffered to a greater degree from wall deposits.

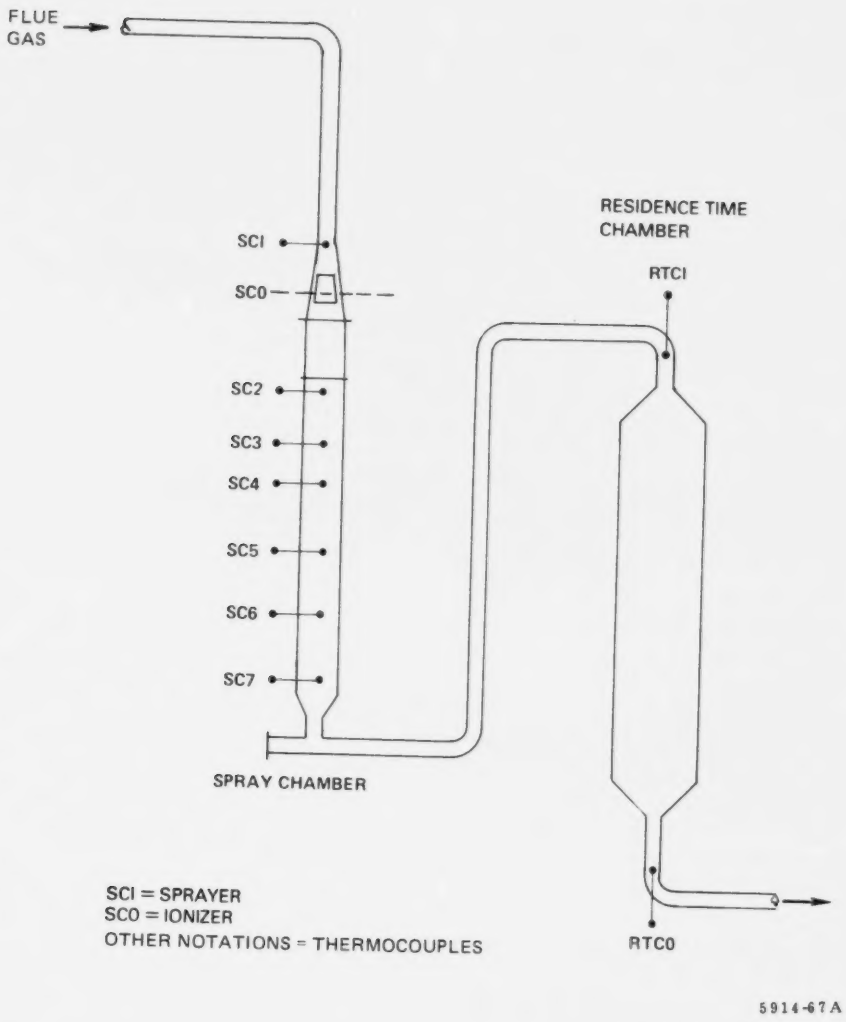

Figure 4-1. Spray chamber and residence time chamber.

Sorbent Concentration and Particle Charging

Determination of the concentration of entrained sorbent particles was made to ensure that an adequate quantity of sorbent was transported from the furnace to the humidifier. Samples were withdrawn at the outlet of the humidifier both with and without particle charging. Quantities of sorbent recovered, relative to the quantities injected, were in the range 40 to 50%, which were typical for this combustor. There was no evidence that particle charging and any resulting particle precipitation significantly lowered the concentration.

Sorbent particles were charged negatively with a sharp-edged disc ionizer, with a diameter of 2.2 in. (5.6 cm), which was located in the centerline of the inlet duct to the spray chamber, as shown in Figure 4-2. Particle charge was determined by collecting particles at the humidifier outlet on an electrically isolated filter and measuring the accumulated charge. With the ionizer at the usual voltage setting, -20 kV, and the water flow rate at a typical value around 4 cm^3/s, the particle charge was in the range 5 to 9 $\mu C/g$, compared to a baseline value of 0.25 $\mu C/g$ with the ionizer not operating.

Water Injection and Droplet Charging

A water spray was introduced with a Sonic Development ST47 two-fluid nozzle. The characteristics of the spray obtained with this nozzle have already been discussed in connection with other humidification studies.

The spray droplets were charged and the quantity of charge was measured with the system shown in Figure 4-3. The nozzle was electrically isolated from ground by channeling the water to the nozzle through plastic tubing; it was energized with a Spellman DC power supply. For measurement of charge, the spray was directed to a bed of steel wool, and the charge thus collected was discharged to ground through a microammeter. The ratio of charge to droplet mass was calculated from the ratio of current to water flow rate. The results were in the range 0.8 to 2.0 $\mu C/g$ at nozzle voltages of 10 to 20 kV. The actual data were obtained with a negative polarity on the nozzle; the specific charge was assumed to be about the same with the positive polarity used for most of the humidification tests.

SO_2 Removal

Tests were performed to compare SO_2 removal by three procedures: sorbent injection without humidification, sorbent injection with humidification but without charging, and sorbent injection with humidification and with charging. In some tests, limestone was injected in the furnace at 2300 °F (1260 °C); in others, hydrated lime was injected downstream from the furnace at 400 °F (200 °C). Firing was always with natural gas; it produced a water vapor concentration of 0.184 mole per mole of dry gas, which was increased by 0.054 mole per mole of dry gas when humidification was in progress (approach to saturation, 20 °F or 11 °C). SO_2 was added from an external source to produce a concentration of 2000 ppm. Changes in SO_2 concentration were used to calculate sorbent utilization; no solids analysis was performed to evaluate utilization by the more direct and reliable approach.

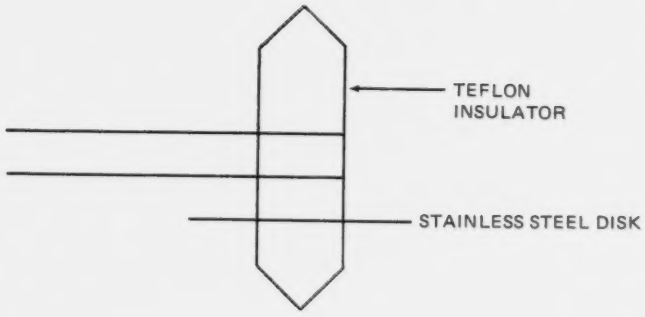

Figure 4-2. Disc-type ionizer.

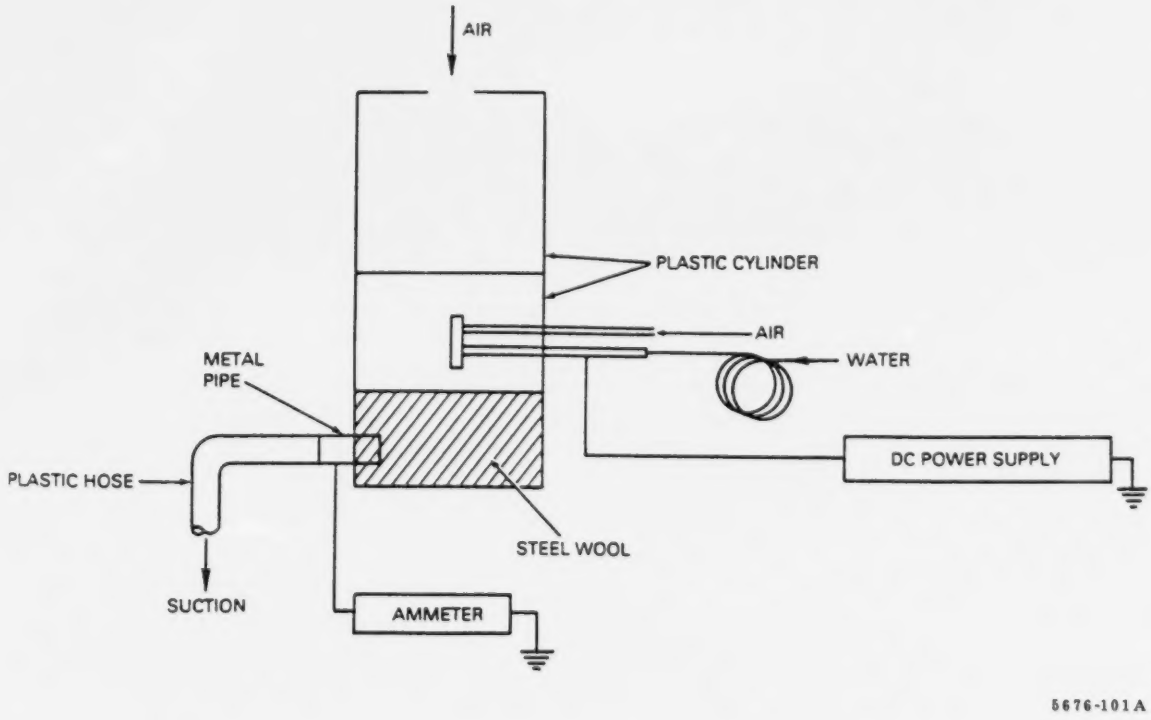

Figure 4-3. Apparatus for drop charging and charge measurement.

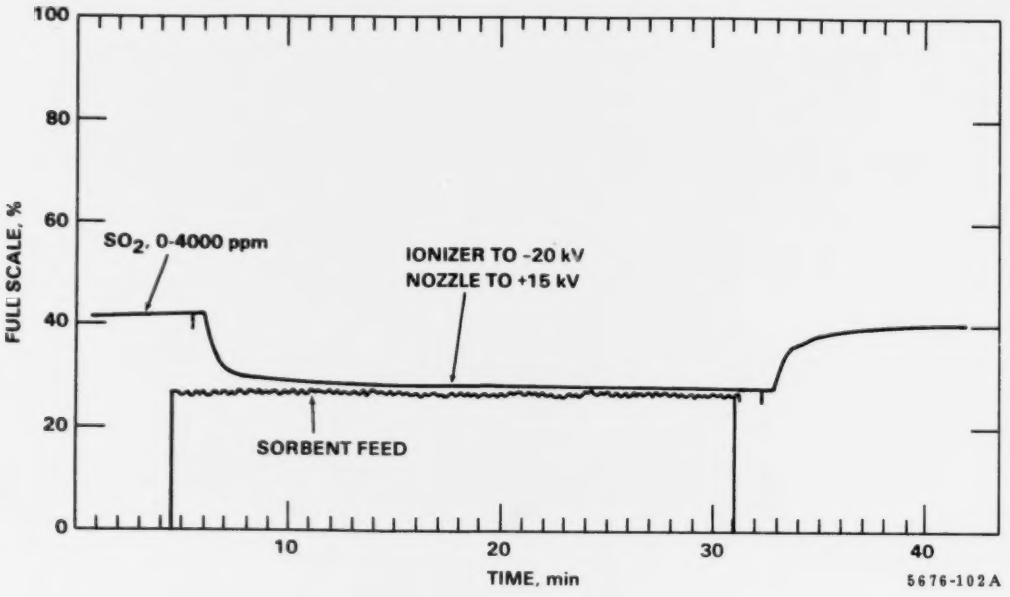

Figure 4-4. Charge augmentation of humidification to enhance SO_2 capture with limestone injection.

For limestone injection at Ca/S = 2.3 without humidification, the reduction in SO_2 concentration was approximately 30%, which corresponds to a utilization of 13%. Again for limestone injected but with humidification, the apparent utilization increased slightly, to about 14%. Both procedures were accompanied by a significant degree of wall reaction. When sorbent injection terminated, the SO_2 concentration did not return to the initial value, and it lagged even more during the experiments with humidification.

The effect of charge augmentation was determined by operating for a time with humidification and then activating the two charging devices. The results of one such experiment as presented in Figure 4-4. Charge augmentation had no observed effect on SO_2 removal. Similar experiments were conducted with a variety of experimental conditions:

- Charging conditions
  - no charging of sorbent particles; negative charging of water droplets

- negative charging of both sorbent and water

- negative charging of sorbent; positive charging of water (the usual conditions).

• Nozzle conditions

- operation with the resonator in place (this device is a small impingement target near the exit)

- operation with the resonator removed, which extended the droplet lifetime.

Under none of these conditions did charging increase the extent of SO_2 removal.

For hydrated lime injected at Ca/S = 1.8 without humidification, sorbent utilization was about 5%. When water was injected, utilization increased to 15%. When water was added and charging was also initiated, no further increase in utilization occurred. Thus, CASH was found equally ineffective for both limestone and hydrated lime.

CONTINUED STUDIES (Cooperative Agreement CR 812811)

Humidification Chamber

The preliminary studies described above were continued after a larger humidification chamber, previously illustrated in Figure 3-1, became available. One of the advantages of the larger chamber, with the diameter increase from 8 in. (20 cm) to 36 in. (91 cm), is a lesser degree of wall deposition of entrained particulate matter. While the further studies were in progress, the need of certain modifications in the sorbent-particle ionizer and the water spray nozzle, with its attendant droplet charging mechanism, became apparent. One further change made in the later studies was the use of solids analysis to obtain a more direct measure of sorbent utilization than that based on the decrease in the SO_2 gas-phase concentration.

The configuration of the humidification chamber and the associated charging devices is shown in Figure 4-5. The sorbent particles were initially entrained in the furnace; they were charged on approaching the inlet to the humidification chamber. The water spray droplets were introduced and ionized immediately inside the inlet. The ionizer shown in the figure for the sorbent is the disc type previously discussed; it was replaced in later work with a wire-pipe charging device. In the figure, the nozzle for introducing the water spray is the Sonic Development ST47 two-fluid nozzle previously described; this nozzle remained in use throughout the work to be described, but the arrangements used for charging the droplet and preventing charge leakage to ground required improvements as the work progressed.

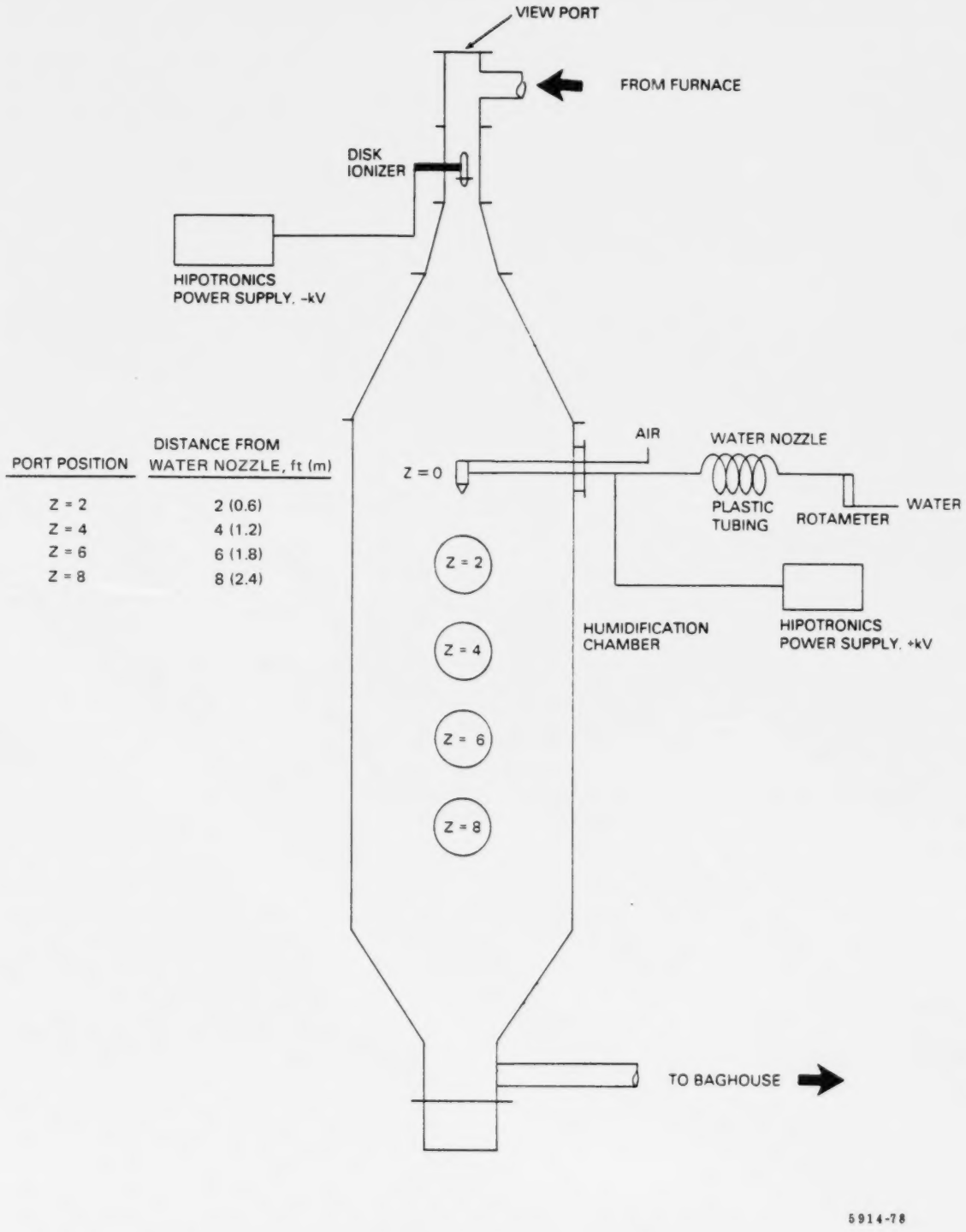

Figure 4-5. Position of ionizer and water nozzle in the pilot combustor.

Charging of Sorbent Particles

The disc ionizer was previously illustrated in Figure 4-2. The 2-in. (5-cm) stainless steel disc was centered within the 4-in. (10-cm) inlet duct to the humidification chamber. It could be charged to voltages within the range -30 to -40 kV, depending upon conditions as will be discussed, but was generally not charged above -15 kV in regular usage. The practical limitation to the maximum ionizer voltage came from high current densities in the sorbent deposits on the adjacent duct walls and the resulting onset of sparking.

Voltage-current data for the disc ionizer operating in clean flue gas from natural-gas firing, both before and after a CASH experiment, are plotted in Figure 4-6. Where the duct walls were free of sorbent deposits in the initial measurements, the ionizer voltage approached -35 kV before sparking occurred, Later, when sorbent deposits were present, sparking occurred at -18 kV. The associated suppression in current was approximately from 1400 μA to 100 μA; obviously, with such a sharp reduction in current, the efficiency of charging of the sorbent particles was severely reduced.

A temporary measure for increasing the ionizer current was to cool the deposits on the duct walls with an external water-cooled jacket. This approach provided some benefit but not the stability in electrical conditions desired.

After a significant volume of work with the disc ionizer had been completed (subsequently detailed in Table 4-2), this ionizer was replaced with a wire-pipe apparatus, which is illustrated in Figure 4-7. Three features of the wire-pipe ionizer favored operation at higher voltages and currents. First, the area of sorbent deposits on the duct walls was much enlarged; this gave substantially lower current densities on the walls for given total currents. The effective length of the 0.125-in. (3.2-mm) discharge wire was 14 in. (35 cm); hence, the adjacent wall area on the 4.26-in. (10.8-cm) duct, was 187 $in.^2$ (1210 cm^2). The estimated area opposite the disc, on the other hand, was approximately 2.5 $in.^2$ or 16 cm^2 (based on an assumed height of 0.4 in. or 1.0 cm). A second favorable feature of the wire-pipe ionizer was the jacketing of the outside wall and cooling with a stream of water. Third, continuous rapping with an air-powered vibrator reduced the quantity of sorbent deposited on the walls.

Voltage-current data of the wire-pipe ionizer are plotted in Figure 4-8. These data were obtained for three conditions with gas firing: neither SO_2 nor sorbent injected; only SO_2 injected, and both SO_2 and sorbent injected. Either additive suppressed the current at the maximum voltage that could be reached; the key result, however, is that the deleterious effects of sorbent were substantially reduced from those apparent with the disc ionizer. With sorbent present, the wire-pipe ionizer was able to operate at nearly 1000 μA, whereas the disc analyzer was restricted to about 100 μA (the wire-pipe device, however, had a current density of only 800 nA/cm^2, whereas the disc ionizer had a current density of 6000 nA/cm^2).

The extent of particle charging was measured as mentioned before, in connection with the initial discussion of the disc ionizer. That is, particles

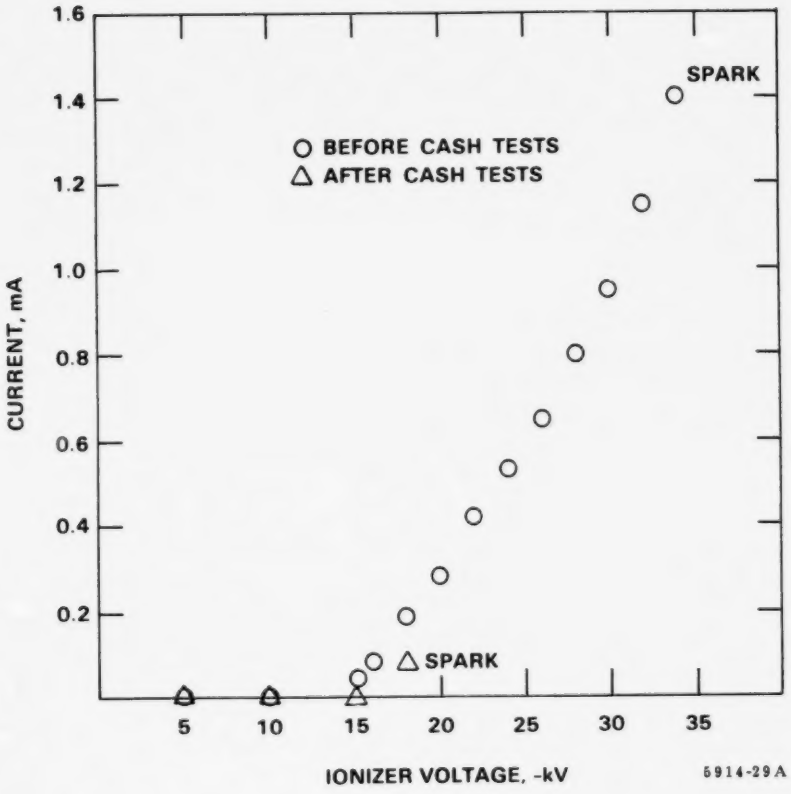

Figure 4-6. V-I curve for disc ionizer. Firing gas at 1.0 x 10^6 Btu/hr (300 kW). Injecting SO_2 to burner.

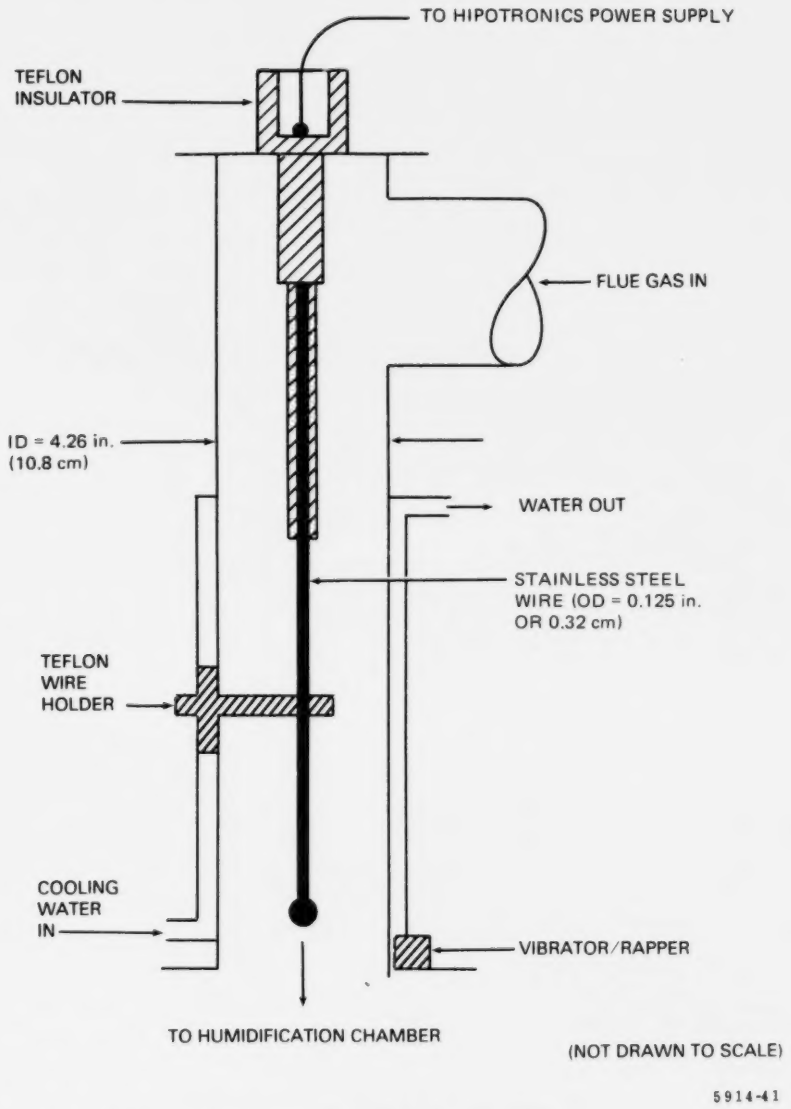

Figure 4-7. Ionization chamber and wire ionizer.

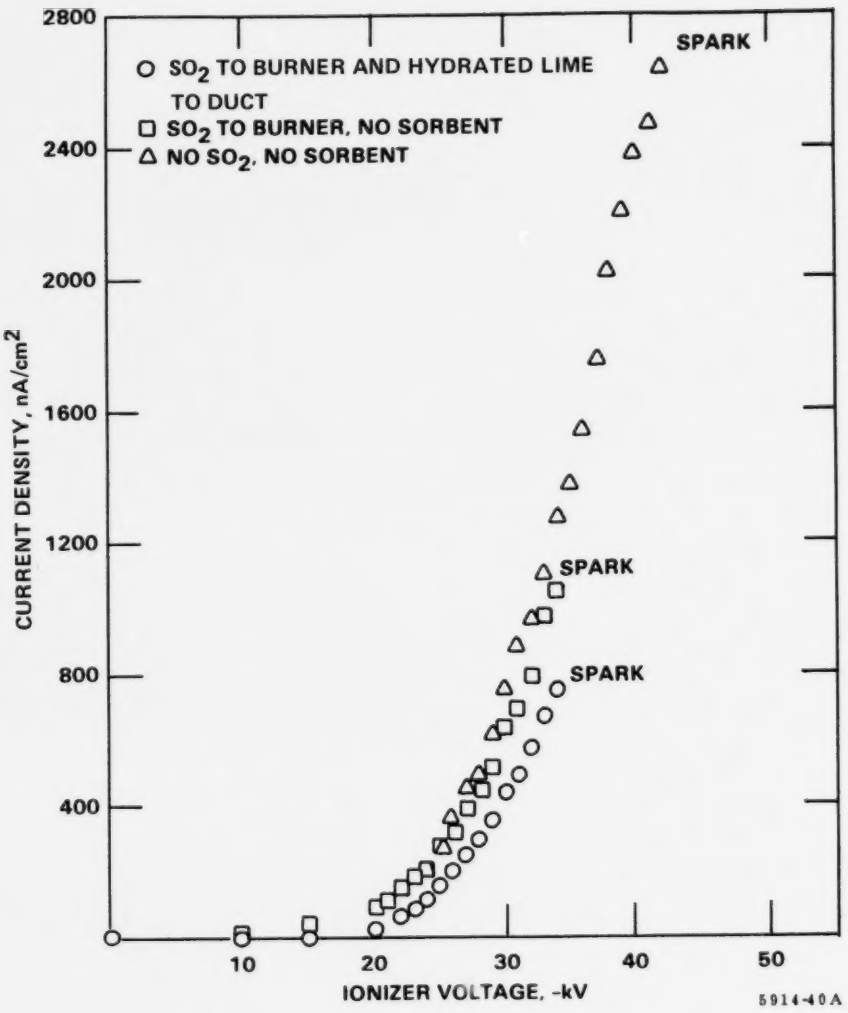

Figure 4-8. Wire-pipe V-I curves with natural gas firing.

were collected on an electrically isolated filter; the total quantity was determined from the increase in filter weight, and the total charge was determined from the integral of current with time, when the accumulated charge was discharged to ground. Illustrative data are given in Table 4-1; the data consist of background charge levels, due to triboelectric charging, and total levels achieved with the ionizer in operation. Charge densities established with combinations of coal ash and sorbent were less than those for sorbent alone (gas firing), presumably because of the larger average particle diameter when ash was present, which led to less efficient charging by the field charging mechanism.

Quantities of solid collected on the filter used for measurements of charge density indicated that electrification of the wire-pipe ionizer caused substantial wall deposition in the humidification chamber. The rate of solids collection on the filter was reduced about 60% when the ionizer was energized.

Table 4-1. Particle Charge Levels from Wire-Pipe Ionizer

Fuel	Site of sorbent injection	Electrical conditions		Charge density, $\mu C/g$
		Voltage, kV	Current density, nA/cm^2	
Gas	Duct	0	0	-0.2
	Duct	-28	170	-4.2
Coal	None	0	0	-0.4
	Furnace	0	0	-0.1
	Duct	0	0	+0.4
	Furnace	-28	200	-1.9
	Duct	-28	330	-1.8

Spraying and Charging of Water Droplets

Water was introduced to the humidification chamber through Sonic Development ST47 two-fluid nozzle. The intent was not only to wet the sorbent particles through charge-augmented collision but to lower the gas temperature to the range 30 to 50 °F (17 to 28 °C) above the adiabatic saturation temperature (around 120 °F or 50 °C). The configuration of the nozzle and the associated droplet-charging apparatus are illustrated in Figure 4-9. This illustration shows the arrangement that finally evolved; features of the illustration that were included in the preliminary arrangement, to provide electrical insulation

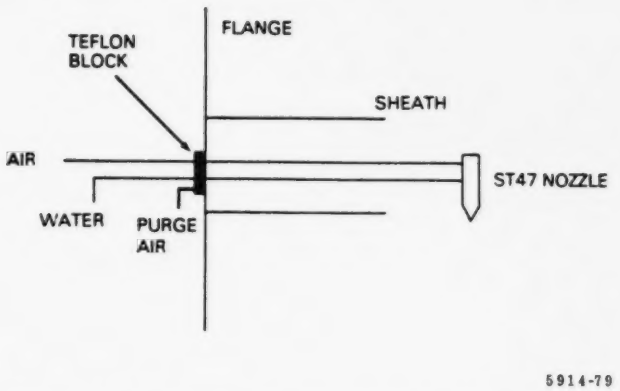

Figure 4-9. Sonic development spray nozzle ST47.

from ground, were the Teflon mounting block, Teflon tubing around the regular water and air tubing to the nozzle, and a long coil of plastic tubing that carried water up to the final inlet to the nozzle.

The initial CASH experiments revealed no benefit from energizing the disc ionizer and the droplet-charging mechanism (see Table 4-2 later). Inspection of the sprayer revealed at that time that several components were wet and suggested that current leakage to ground had nullified attempts to charge the droplets. Thereafter, two steps were taken to prevent this problem. First, a means was provided to maintain a stream of purge air around the air and water tubes inside the chamber; still, evidence of an electrical short was encountered. Next, a stainless steel sheath was inserted around the air and water tubes inside the chamber; this final arrangement seemed to satisfy the requirements.

The charge density in the water droplets was determined with the arrangement previously shown in Figure 4-3. The results thus obtained with two operating variables — the water flow rate to the nozzle and the nozzle voltage — are plotted in Figure 4-10. Typical operating conditions were a water flow rate of 350 cm^3/min and a voltage of +5, +10, or +15 kV. Thus, according to Figure 4-10, the average droplet charge was in the range from about 0.2 to 1.0 $\mu C/g$.

SO_2 Removal with the Disc Ionizer (Gas Firing)

Throughout the experiments with the disc ionizer, the furnace of the combustor was fired with natural gas at the rate of 1 x 10^6 Btu/h (300 kW). SO_2 was provided from an external source; it was injected through the burner to produce a concentration of 2000 to 2200 ppm. Longview $Ca(OH)_2$ was injected in the furnace at a temperature of approximately 2200 °F (1200 °C) to produce a

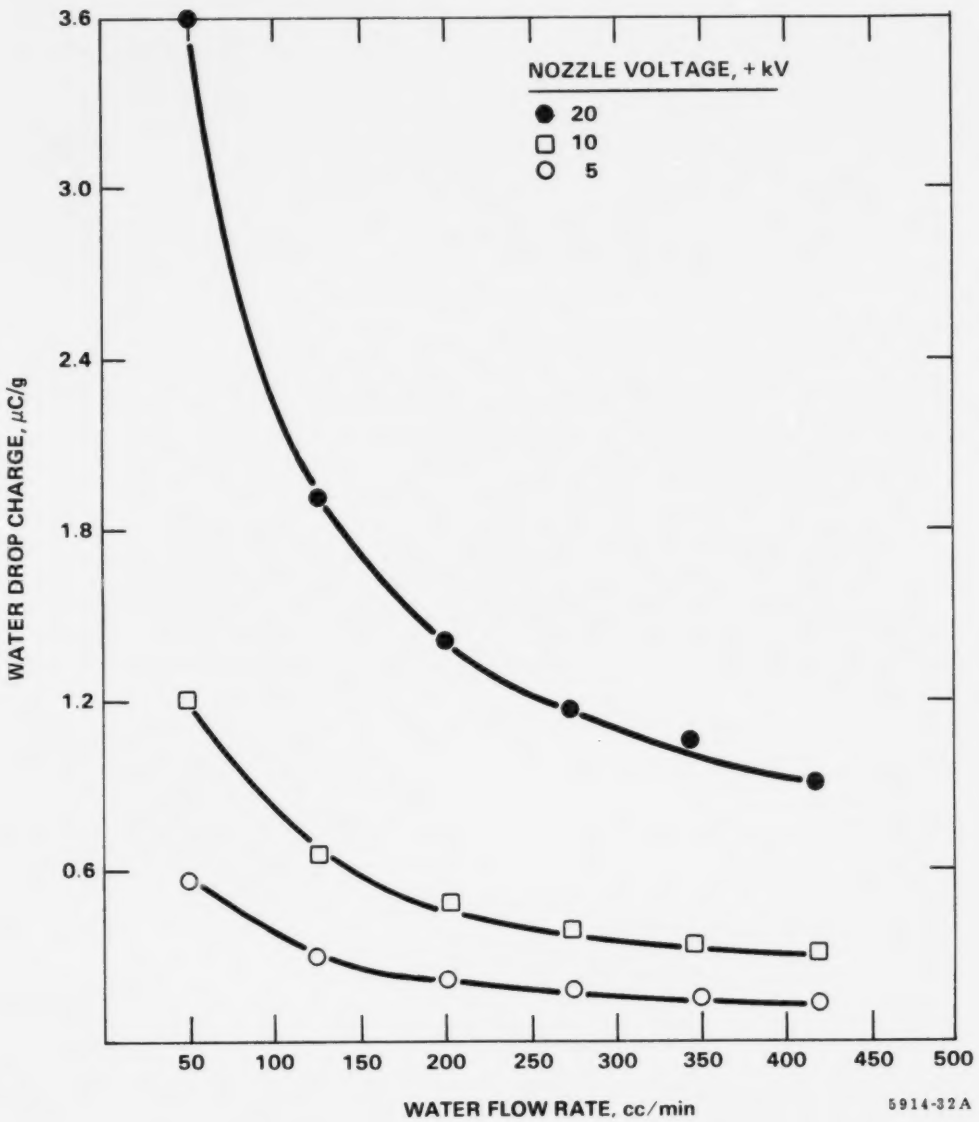

Figure 4-10. Effect of water flow rate and nozzle voltage on the average water droplet charge.

Ca/S ratio of about 1.6. Gas-stream temperatures downstream from the furnace were regulated to the range 300 to 350 °F (150 to 175 °C) at the inlet to the humidification chamber.

The results on SO_2 removal with the disc ionizer and the water spray nozzle in various arrangements are listed in Table 4-2. The data include the results of baseline determinations of the removal of SO_2 when neither the sorbent particles nor the water droplets were charged (removal under these conditions, of course, was the result primarily of furnace reaction). The data also include determination of SO_2 removal after charging had been discontinued; these results indicate the degree to which increasing wall deposition may have influenced the apparent effects of charging. The data include scattered indications that charging increased SO_2 removal but, on balance, indicate that the charges were primarily a temporal effect, due to increased wall deposits, not the effect of charging itself. The magnitude of drifts with time is visually apparent in Figure 4-11.

A limited number of experiments to determine the increment in sorbent utilization due specifically to charging were performed. These were accomplished with a quench probe for removing solids in a heated, diluted stream, which ensured that reaction between the solids and SO_2 in gas phase would cease during the extraction process. Representative results that were thus obtained are tabulated below:

No charging S/Ca mole ratio = 0.27

Ionizer at -9 kV, nozzle at +5 kV S/Ca mole ratio = 0.26

These data indicate that any effect of charging was small enough to lie inside the range of experimental error.

SO_2 Removal with the Wire Pipe Ionizer (Coal-Firing)

After the wire-pipe ionizer replaced the disc ionizer, all CASH experiments were performed with coal firing rather than gas firing. The Edgewater demonstration coal (Boich mine, Pittsburgh No. 8 seam) was burned at 1.0×10^6 Btu/h (300 kW). $Ca(OH)_2$ was injected either in the furnace at 2200 °F (1200 C°) or a duct at 400 °F (200 °C). The extent of sorbent utilization was calculated from either the change in SO_2 concentration or the analysis of the suspended solids.

The data obtained during these experiments are presented on Table 4-3. To say that energization of the ionizer and the nozzle did not increase sorbent utilization is a conservative observation. To say, on the other hand, that energization actually decreased utilization for duct-injected sorbent is a fair observation based on the gas-phase data with duct injection. A possible rationalization of the latter observation is that much of the sorbent was removed from the gas stream and deposited on the walls of the humidification chamber and, hence, made relatively ineffective for SO_2 removal. As previously stated, data from determination of sorbent charge density gave a strong indication of sorbent precipitation on the chamber walls.

Table 4-2. Removal of SO_2 During Experiments with the Disc Ionizer

Spray nozzle configuration[a]	Approach to saturation, °F(°C)	Charging voltage, kV		Removal of SO_2, %		
		Ionizer	Nozzle	Baseline	During charging	After charging
A	30 (17)	0	0	60.5	-	-
A	-	-10	+.5	51.9	52.1	-
B	40 (22)	-10	+.5	48.2	54.4	-
B	35 (19)	0	0	44.9	-	-
C	45 (25)	-10	+5	41.9	46.6	48.3
C	45 (25)	-10	+10	48.3	50.0	51.7
C	45 (25)	-10	+15	51.7	53.5	55.1
C	45 (25)	-10	+15	55.2	56.2	-
C	45 (25)	-13	+10	48.6	51.7	54.8
C	45 (25)	-13	+15	54.8	55.4	56.0
C	45 (25)	-13	+5	56.1	60.0	61.9

A. With neither purge air nor protective sheath.
B. With purge air but not sheath.
C. With purge air and sheath.

Table 4-3. Removal of SO_2 During Experiments with the Wire-Pipe Ionizer (Coal Firing)

Site of Sorbent Injection	Approach to Saturation, °F(°C)	Voltage, kV		Sorbent utilization			
				SO_2 removal		Solids analysis	
		Ionizer	Nozzle	Baseline	CASH	Baseline	CASH
Furnace	60 (33)	0	0	37.2		34.4	
	60 (33)	-28	+20		31.2		34.4
	55 (31)	-28	+20	37.9	38.2		
	45 (25)	-28	+20	34.1	34.4		
Duct	170 (94)[a]	0	0	3.0			
	55 (31)	-24	+20		11.8		11.7
	45 (25)	0	0	15.7		13.4	
	45 (25)	-24	+20		10.2		13.6
	35 (19)	0	0	17.5			
	35 (19)	-26	+20		16.4		15.6
	20 (11)	0	0	19.2		17.2	
	20 (11)	-24	+20		17.3		16.3

a. No water added.

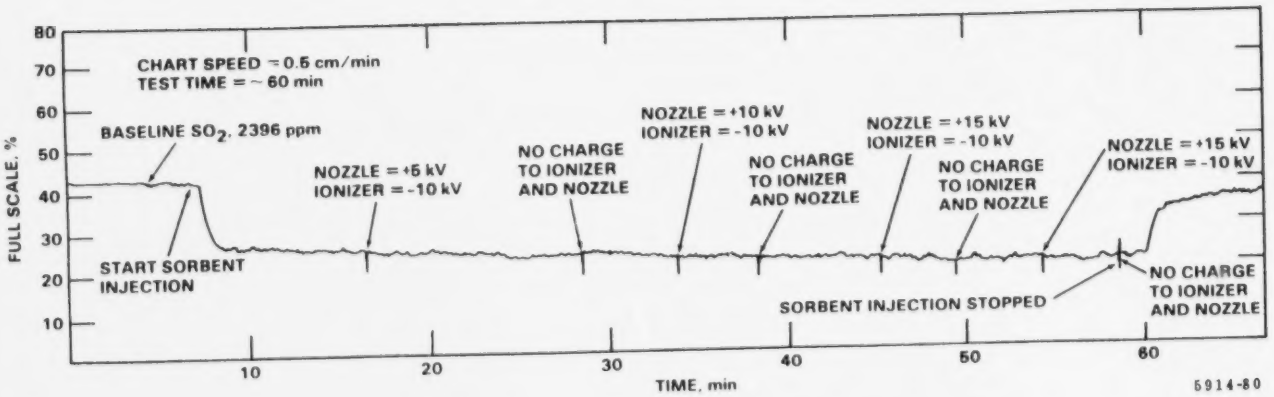
CHART SPEED ~ 0.5 cm/min
TEST TIME = ~ 60 min
BASELINE SO_2, 2396 ppm
START SORBENT INJECTION
NOZZLE = +5 kV
IONIZER = -10 kV
NO CHARGE TO IONIZER AND NOZZLE
NOZZLE = +10 kV
IONIZER = -10 kV
NO CHARGE TO IONIZER AND NOZZLE
NOZZLE = +15 kV
IONIZER = -10 kV
NO CHARGE TO IONIZER AND NOZZLE
NOZZLE = +15 kV
IONIZER = -10 kV
SORBENT INJECTION STOPPED
NO CHARGE TO IONIZER AND NOZZLE
FULL SCALE, %
TIME, min
5914-80

Figure 4-11. Trace of SO_2 concentration in pilot furnace during CASH experiments.

CONCLUSIONS

In neither the preliminary studies of CASH under Cooperative Agreement CR 811683 nor in the further studies under Cooperative Agreement CR 812811 was any favorable effect on sorbent utilization discerned. The reasons for this disappointing result are not clearcut. One possible explanation, however, is that the attractive force between oppositively charged sorbent particles and water droplets is small; it decreases with the square of the separating distance and is small in comparison with other electrical forces except when the separating distance is of the order of the particle-dimensions. The other electrical forces arise from the lack of precise electrical balance between positive and negative charges. In the absence of zero as a net charge in the cloud of particles and droplets, an electrical force operates on each, bringing about a separation and deposition on the container walls.

SECTION 5

LABORATORY STUDIES OF WATER-VAPOR ADSORPTION BY $Ca(OH)_2$ WITH AND WITHOUT ADDITIVES

INTRODUCTION

The results of experimental studies previously discussed in Section 3 make it apparent that $Ca(OH)_2$ is not efficiently activated as a low-temperature SO_2 sorbent by water vapor alone. The experimental data show, on the other hand, that $Ca(OH)_2$ particles that have been physically wetted, by either collision with water droplets or by slurrying with bulk water, are reasonably effective in reacting with SO_2. The CASH process represented one approach (however, unsuccessful) for augmenting the wetting of $Ca(OH)_2$ particles. The use of water-attracting additives to $Ca(OH)_2$ is another means of inducing the wetting of $Ca(OH)_2$ particles; this is an approach that has been studied by various investigators, as described below.

This section presents the results of laboratory studies to determine quantitatively the ability of $Ca(OH)_2$ to attract water from the vapor state. Most of the measurements were made with $Ca(OH)_2$ that had been modified with additives; reference measurements, however, were made with unmodified $Ca(OH)_2$. The results of these studies are portrayed as water-vapor adsorption isotherms, which are plots of the weight ratio of adsorbed water to dry solid as a function of the relative partial pressure of water vapor, p/p^0, at a specified temperature (in other words, the ratio of the actual partial pressure to the value at saturation). All of the data presented are for a temperature of 140 °F (60 °C), which is within the range to be expected when flue gas is humidified and cooled with a water spray. This temperature represents an approach to adiabatic saturation of about 18 °F (10 °C), assuming flue gas initially at 300 °F (150 °C) with a water vapor concentration of about 7%.

BACKGROUND

Water-Attracting Additives in Sorbents

Water-attracting additives in calcium-based sorbents have been investigated in recent years for application in both spray dryers and low-temperature duct-injection processes for dry sorbents (1-5). In each of these applications, the intent is to extend the operating time during which the sorbent remains physically wet and thus more reactive with SO_2. Frequently, the additives have been described as deliquescent, a term which implies that the additives have such a high affinity for water vapor that they cause condensation into a solution of the additive. A strict consideration of the additives that have produced beneficial results reveals, however, that the degree of deliquescence varies widely and suggests that some of the compounds are not literally deliquescent under the conditions of use. This investigation of water-vapor adsorption isotherms of $Ca(OH)_2$-additive mixtures has confirmed this concept and has shown further that an additive that is deliquescent when pure under the

selected humidity conditions may not be deliquescent when combined with $Ca(OH)_2$ under those same conditions.

Several investigators have identified sodium salts as promising additives in $Ca(OH)_2$. Yoon et al.(6), for example, have reported that all members of the following family of sodium salts produced beneficial effects with respect to SO_2 capture: NaOH, NaCl, $NaNO_3$, Na_2CO_3, and Na_2SO_3. The difference in deliquescence of the first two members of this series is apparent in Figure 5-1, which depicts the suppression in vapor pressure of water at 60 °C that results from the dissolution of each compound. For the saturated solution of NaCl, the value of the relative partial pressure, p/p^0 (the ratio of the partial pressure from the solution to that of pure water), is reduced to 0.749 (7,8). For the saturated solution of NaOH, on the other hand, the value of p/p^0 is reduced to a value below 0.01 (9). Thus, NaCl is deliquescent at 60 °C only if p/p^0 reaches or exceeds 0.749 (relative humidity, $\geq$ 74.9%), whereas NaOH is deliquescent at 60 °C through a range of much lower p/p^0 values, beginning at below 0.01 (relative humidity, <1%).

The thresholds of deliquence of all five of the sodium salts (7-10) are compared in Figure 5-2. The primary factor responsible for the differences in p/p^0 at saturation is the variation in solubility. Clearly, some factor other than the tendency to deliquescence must account for the grouping of all five salts as effective additives.

Ruiz-Alsop and Rochelle (5) have recognized that deliquescence is not the only controlling property of additives that improve the ability of $Ca(OH)_2$ to react with SO_2. They found that the most promising additives among the compounds they studied were LiCl, KCl, NaCl, NaBr, and $NaNO_3$. Of those, only LiCl can be considered a classical deliquescent salt; it dissolves in atmospheric moisture at 60 °C if p/p^0 is as low as 0.10 (9,11), whereas the other four do so only if p/p^0 exceeds 0.65 (8). The authors were only able to speculate, however, about other mechanisms that may be involved in the activation of the $Ca(OH)_2$-SO_2 reaction.

Water-Vapor Adsorption Isotherms on Sorbents

There appears to be no published literature on the measurement of water-vapor adsorption isotherms on $Ca(OH)_2$ modified with water-attracting additives. Glasson (12), however, studied the uptake of water vapor in association with the chemical reaction between water vapor and CaO to product $Ca(OH)_2$. Glasson concluded that the chemical process stopped at $Ca(OH)_2$; there was no formation of the postulated hydrate $Ca(OH)_2 \cdot 1/2\ H_2O$. In addition, Klingspor, et al. (13) investigated the adsorption of water vapor by various $Ca(OH)_2$ and $CaCO_3$ specimens ranging in specific surface area from 2 to 26 m^2/g and depicted the results with a Type II adsorption, as illustrated in Figure 5-3. Plotting the relative quantity of water adsorbed as the weight ratio of water to substrate gave a family of curves; plotting weight of water per unit of surface area, however, gave a single isotherm, as depicted in Figure 5-3.

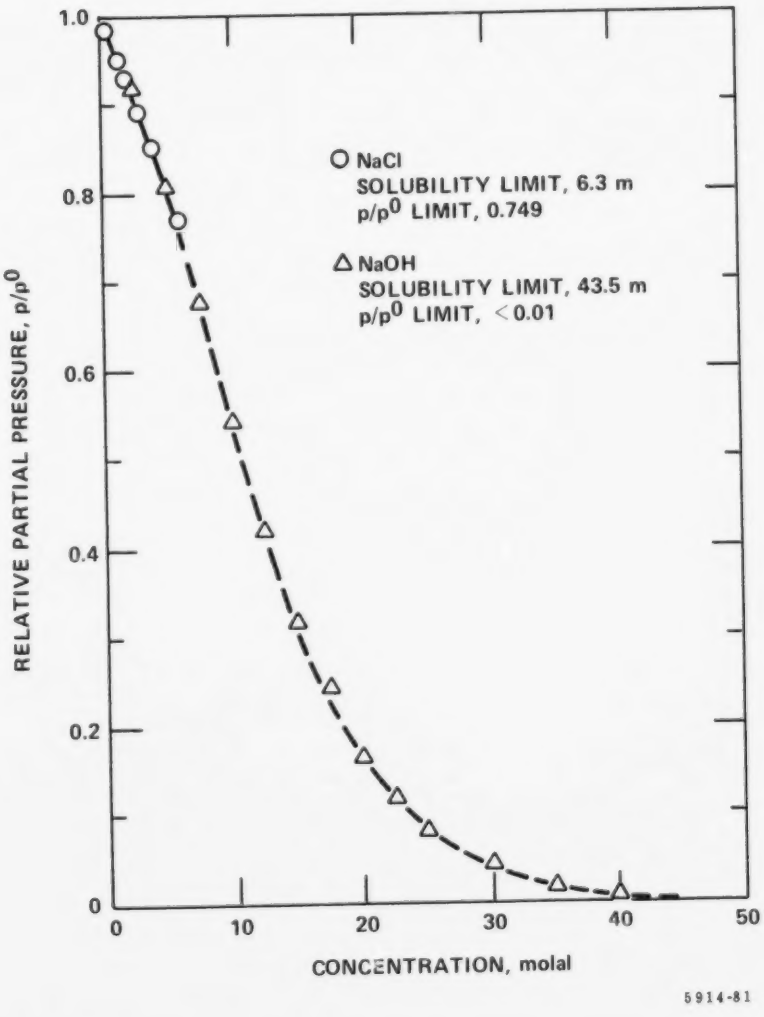

Figure 5-1. Water vapor suppression by dissolved NaCl or NaOH at 60°C.

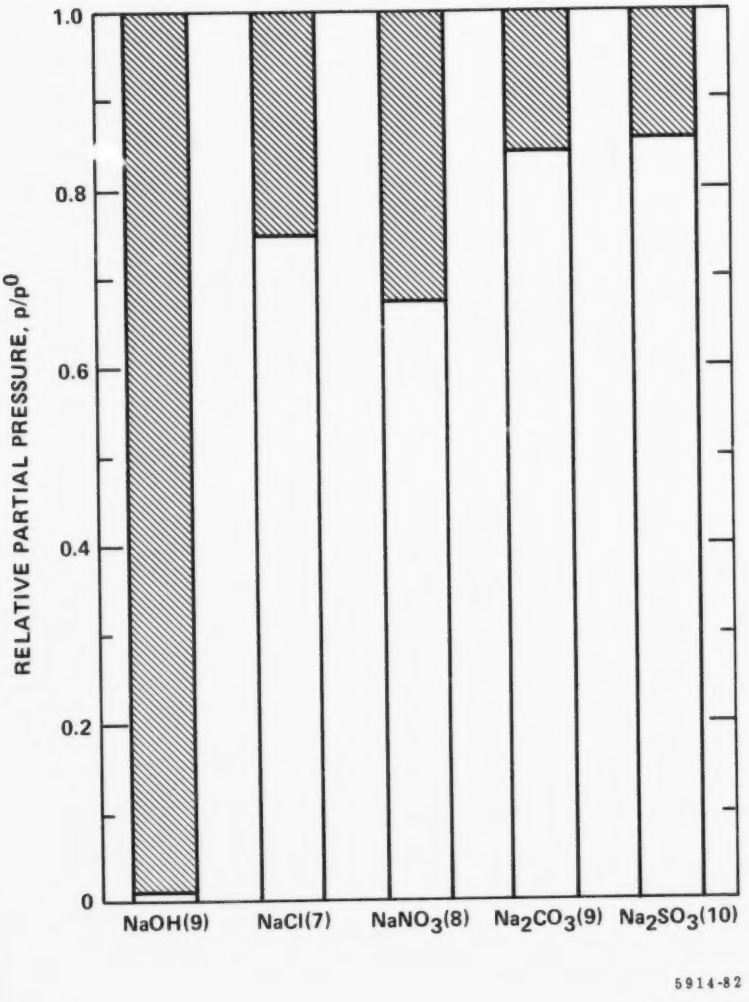

Figure 5-2. Ranges of deliquescence of various sodium compounds at 60°C (deliquescence occurs in shaded range of p/p^0).

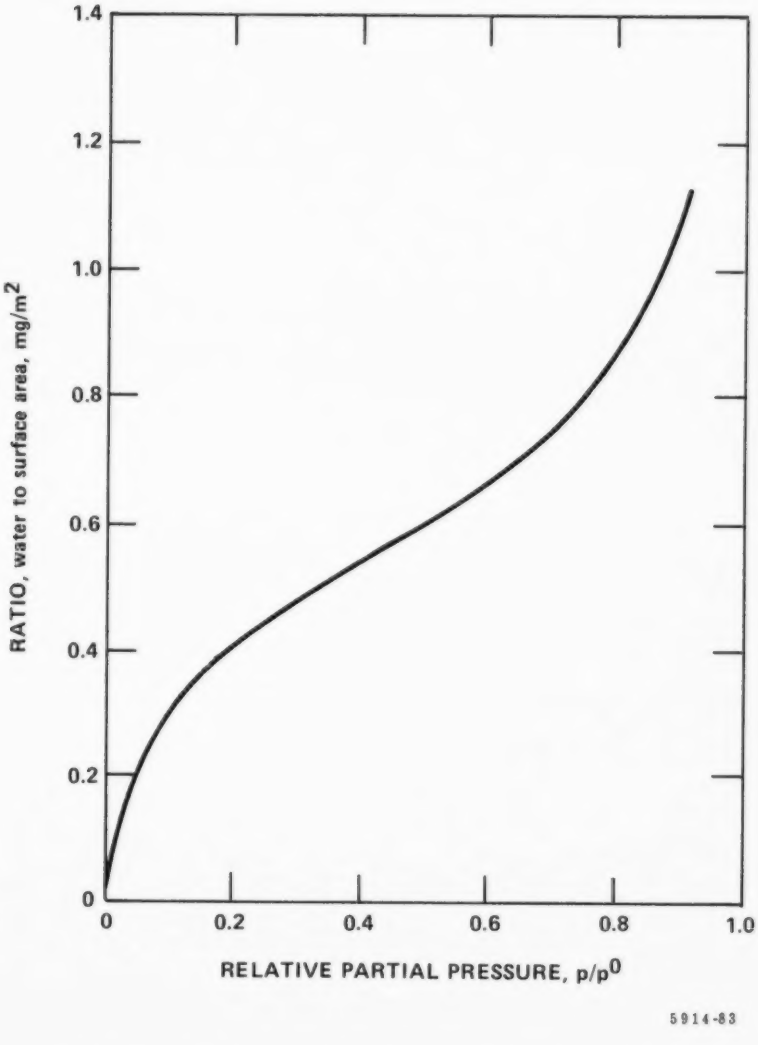

Figure 5-3. Water vapor adsoption on $Ca(OH)_2$ and $CaCO_3$ as reported by Klingspor et al. (13).

EXPERIMENTAL METHODS

Measurement of Adsorption Isotherm

The data of Glasson (12) and Klingspor et al. (13) were obtained with gravimetric devices that directly weighed the quantity of water adsorbed. The data in this laboratory were obtained by a fundamentally different procedure, based on an Accusorb 2100 surface area analyzer purchased from the Micrometrics Instrument Corporation. Fundamentally, this apparatus gives a measurement of the total pressure of a gas in equilibrium with a solid in a system of controlled temperature. Usually, the only gaseous species present is the one whose adsorption isotherm is measured; this was water vapor in the present instance. The remaining data consisted of the weights of the solid materials before and after equilibration with water vapor.

A schematic diagram of the Accusorb 2100 is given in Figure 5-4. This illustration shows four sample containers that can be simultaneously equilibrated at a given temperature with a selected partial pressure of the adsorbate. In this work, the adsorbate (water vapor) was supplied by a reservoir of liquid water attached at one of the sample locations. The possibility of equilibrating three solid samples remained; however, the properties of the different types of solid samples to be studied varied significantly and, thus, their adsorption properties were measured independently.

The apparatus used in these studies was modified from the usual commercial form to raise the maximum temperature of the gas/solid equilibrium system that can be maintained. In this work, 65 or 70 °C could be reached and maintained with difficulty; in most of the experiments, 60 °C was a more practical limit. In comparison, in the unmodified instrument, 40 °C is the upper limit for experimental work. The changes in the instrument included a thermostatic chamber to keep the samples holder and water reservoir constantly at the temperature selected for measurement. They also included heat-traced and insulated shielding for vapor communication lines in the chassis of the instrument, to keep the water vapor above its dew point at all locations.

The procedure used for measurements of water vapor adsorption consisted of the following steps:

- The solid sample was exhaustively dried under high vacuum at 150 °C. It was weighed before and after drying; the latter weight was used as the basis for calculating the relative weights of water uptake.

- The sample and the water reservoir were then heated in the Accusorb to 60 °C (the usual experimental temperature). The sample was equilibrated at the lowest relative pressure of water vapor that was of interest — say, $p = 10$ mmHg or $p/p^0 = 0.07$. This objective was achieved by momentarily opening the stopcock from the water reservoir into the manifold, which was connected to both the sample container and the pressure transducer. Once

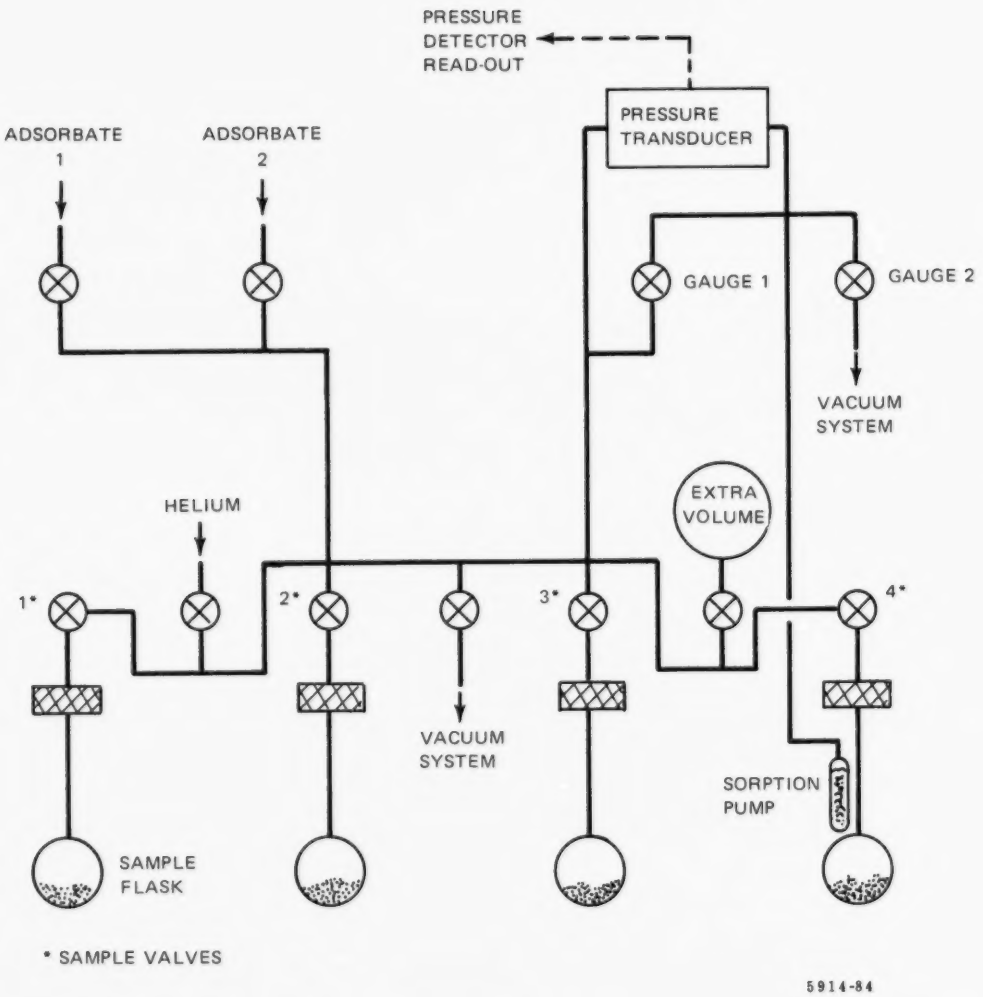

Figure 5-4. Schematic diagram of manifold, gas and sample attachment and pressure measuring system of the Accusorb 2100 Analyzer.

the water reservoir was isolated from the reservoir, the pressure decreased rapidly as the result of vapor uptake by the solid and slowly approached an equilibrium value. To reach the desired p/p^0 value, by supplying the required amount of water to both the couple and the vapor space, the reservoir sometimes had to be opened and closed several times. Once equilibrium was attained, the sample container was detached and the sample weight was determined. The increase over that recorded after the initial drying was an approximate measure of the quantity of water adsorbed.

- The above steps were repeated with progressive increases in the p/p^0 value until finally a p/p^0 value between 0.9 and 1.0 was established. The final measurement completed determination of the ascending limb of the adsorption isotherm. Reversing the direction of changes in p/p^0 gave the descending limb.

Preparation of Additive-Modified $Ca(OH)_2$

Two forms of commercial lime products were purchased from Longview Lime Division of Dravo Lime Company at Saganaw, Alabama. One of these products was $Ca(OH)_2$ and was experimentally studied without any modification. The other product was quicklime, CaO, from which the $Ca(OH)_2$ had been manufactured by hydration. The CaO was converted to $Ca(OH)_2$ in our laboratory in a hydration medium that contained one of the additives of interest. The $Ca(OH)_2$ had a mass-medium diameter of about 2 μm; it had a specific surface area of about 20 m^2/g. The CaO was pulverized before use and fractionated by sieving; only the fraction passing a 28-mesh screen was used for the hydration experiments. The screened fraction had a mass-medium diameter of 17 μm and a specific surface area of 2.2 m^2/g.

Hydrates of CaO and each of the additives were produced in a Ross ribbon blender. Approximately 15 lb (6.8 kg) of pulverized CaO was treated with 8.2 lb (3.7 kg) of water containing the selected quantity of additive in solution. The reaction was carried out in an open environment; the excess of water (about 70% over that required for the chemical transformation) was vented as steam and yield a dry, freely-flowing powdered product.

The mole ratio of additive to CaO charged to the reactor was controlled to give additive/$Ca(OH)_2$ mole ratios as follows:

$LiCl/Ca(OH)_2$	0.10
$NaCl/Ca(OH)_2$	0.10
$Na_2CO_3/Ca(OH)_2$	0.05
$CaCl_2/Ca(OH)_2$	0.05

EXPERIMENTAL RESULTS*

Adsorption versus Desorption

Adsorption data for the $NaCl/Ca(OH)_2$ system that were obtained with increasing and decreasing values of p/p^0 are depicted in Figure 5-5. Hysteresis effects of the type illustrated here were always observed with additive-modified $Ca(OH)_2$, whenever both ascending and descending limbs of the adsorption isotherms were determined. Some evidence of these effects were also observed with unmodified $Ca(OH)_2$, but they were much less pronounced.

Hysteresis is a commonly observed feature of adsorption isotherms, especially when condensation of the adsorbate occurs (as here). Various theoretical interpretations for the effect have been offered; different views exist on whether data for the ascending or descending limb of the isotherm should be used for interpretative purposes, such as determining pore sizes. No attempt was made to explain the hysteresis in the present study. The primary emphasis in the recording and illustration of data was on the ascending mode, since the phenomenon to which the data relate is the adsorption of water vapor, not desorption.

Observed Effects of Additives

Data from representative experiments on modified and unmodified $Ca(OH)_2$ are listed in Table 5-1. The influence of the several additives on the adsorption of water vapor is shown graphically in Figure 5-6. The maximum uptake of water by unmodified $Ca(OH)_2$ is represented by a weight fractional increment $\Delta g/g = 0.043$ (i.e., a weight addition of about 4.3%) at $p/p^0 = 0.94$. The most dramatic effect of an additive occurred with LiCl, which gave a weight increment more than 10 times as large — $\Delta g/g = 0.52$ — near the same value of p/p^0. The effects of the several additives are discussed in the following paragraphs.

LiCl. Enhancement of water uptake by this salt evidently extended at least throughout the region of p/p^0 values measured (0.20-0.92). Onset of deliquescence by LiCl is said to occur at $p/p^0 = 0.10$ (9). The data obtained are, therefore, qualitatively as expected.

NaCl. The effect of this salt became evident only when the p/p^0 reached a value around 0.75 but, thereafter, approached the effect of LiCl. NaCl becomes deliquescent only at $p/p^0 = 0.749$ (8); thus, the data for this salt, like the data for LiCl, are qualitatively as expected.

Na_2CO_3. This additive had far less effect than expected. The surprise arose not from any expectation of strong deliquescence of Na_2CO_3 itself; it arose instead from the failure of the compound to behave effectively as NaOH rather than Na_2CO_3.

*All adsorption data cited are for 60 °C.

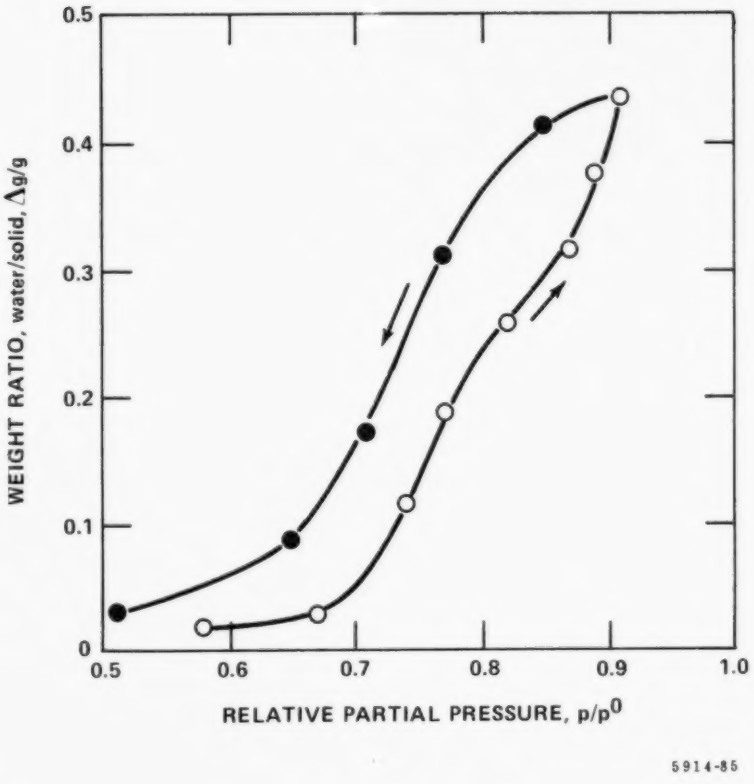

Figure 5-5. Adsorption and desorption isotherms for $NaCl/Ca(OH)_2$ system at 60°C.

TABLE 5-1. EXPERIMENTAL DATA ON THE UPTAKE OF WATER VAPOR BY $Ca(OH)_2$-CONTAINING SYSTEMS AT 60 °C

Additive	Relative partial pressure, p/p^0	Weight ratio, water/solid, $\Delta g/g$
None	0.60	0.016
	0.75	0.020
	0.84	0.026
	0.90	0.035
	0.94	0.043
LiCl	0.20	0.055
	0.40	0.093
	0.58	0.150
	0.65	0.176
	0.76	0.254
	0.80	0.285
	0.87	0.400
	0.92	0.520
NaCl	0.58	0.016
	0.67	0.028
	0.74	0.113
	0.75	0.150
	0.77	0.187
	0.82	0.255
	0.87	0.314
	0.89	0.375
	0.91	0.434
Na_2CO_3	0.60	0.029
	0.68	0.096
	0.76	0.121
	0.83	0.160
	0.88	0.195
	0.92	0.226
$CaCl_2$	0.60	0.028
	0.71	0.118
	0.73	0.120
	0.80	0.158
	0.86	0.194
	0.91	0.240
	0.93	0.258

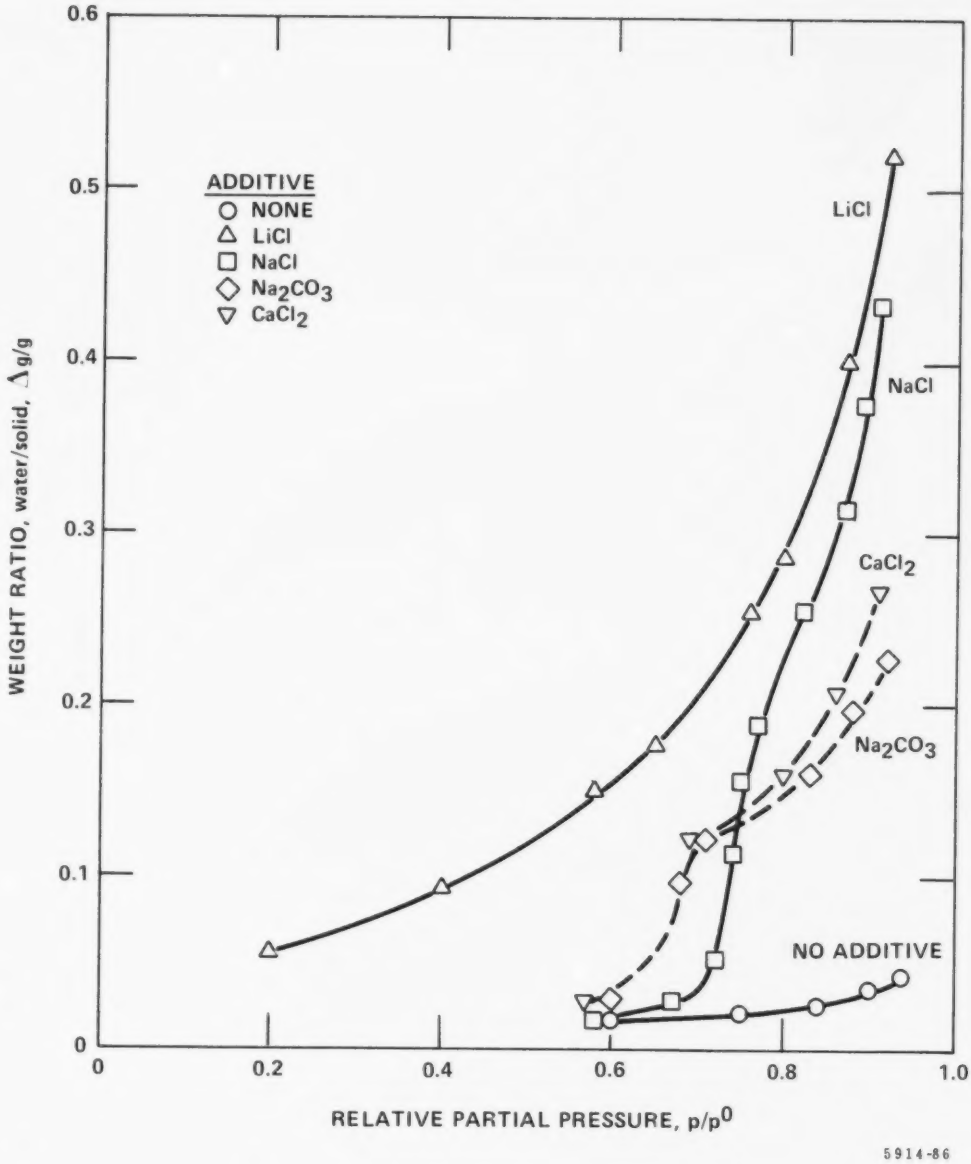

Figure 5-6 Adsorption isotherms for $Ca(OH)_2$ with and without additives at 60°C.

In the hydration medium used for preparing the sample, occurrence of the following double-decomposition reaction was expected:

$$Na_2CO_3(aq) + Ca(OH)_2(s) \rightarrow 2NaOH(aq) + CaCO_3(s)$$

$CaCO_3$, being far less soluble than $Ca(OH)_2$, should have changed the dissolved sodium compound from the carbonate to the hydroxide. NaOH, unlike Na_2CO_3, is strongly deliquescent, having its onset of deliquence at p/p^0 value of below 0.01 (9).

$CaCl_2$. This additive also was surprisingly ineffective. Its onset of deliquescence is at $p/p^0 = 0.17$ (9). Nevertheless, no effect on water uptake was apparent except when p/p^0 approached 0.7. Even at $p/p^0 = 0.9$, the effect of $CaCl_2$ was less than that of either NaCl or LiCl.

Observed Effects versus Predicted Effects of Additives

The foregoing discussion indicates that a prediction can be made of the range of p/p^0 values where the deliquescence of an additive enhances water uptake, provided of course that this additive acts independently from the $Ca(OH)_2$ substrate. In actuality, predictions of the extent of water uptake can also be made on a quantitative scale throughout the range where deliquescence is expected. Predictions of the latter type are made on the basis of the thermodynamic data for aqueous solutions of the additive; such predictions are illustrated below for the system LiCl/water.

Activity coefficients of water in LiCl/water solutions were calculated from the osmatic coefficients of Gibbard and Scatchard (11); the results are listed in the second column of Table 5-2. The weight of water per mole of LiCl at each solution concentration was then calculated (third column); finally, the weight of water per unit weight of the experimental $LiCl/Ca(OH)_2$ mixture, containing 10 moles of $Ca(OH)_2$ per mole of LiCl, was calculated (fourth column). With the data in the first and fourth columns of Table 5-2 combined, Curve A in Figure 5-7 was obtained. This curve predicts the effect of LiCl on water uptake by the mixture. The prediction is completed by extrapolation of the curve to $p/p^0 = 0.10$, where there is the onset of deliquescence at a concentration of 24 molal (9). The discontinuity at $p/p^0 = 0.10$ reflects the hypothetical transition from nonadsorbing anhydrous LiCl below this humidity level to saturated aqueous LiCl above this level. A similar treatment of data for the $NaCl/H_2O$ system (7) yielded Curve B in Figure 5-7.

Comparison of the calculated curves, A and B, with the experimental data for the systems $LiCl/Ca(OH)_2$ and $NaCl/Ca(OH)_2$, which are plotted in Figure 5-7, indicates that success of the predictive method was reasonably satisfactory for both systems. In particular, Curve B depicts reasonably well the abrupt rise in the observed extent of adsorption by the $NaCl/Ca(OH)_2$ mixture near $p/p^0 = 0.75$.

TABLE 5-2. WATER ACTIVITY AND PARTIAL PRESSURE FOR LiCl SYSTEMS BASED ON GIBBARD AND SCATCHARD DATA (11)

Concentration, molal	Water activity[a]	Ratio, g H_2O per mol LiCl[b]	Ratio, g H_2O per g mixture[c]
1.0	0.964	1000.00	0.7833
2.0	0.922	500.00	0.6383
3.0	0.874	333.33	0.4255
4.0	0.819	250.00	0.3191
5.0	0.759	200.00	0.2553
6.0	0.695	160.67	0.2128
7.0	0.630	142.86	0.1824
8.0	0.565	125.00	0.1596
9.0	0.502	111.11	0.1418
10.0	0.445	100.00	0.1277
12.0	0.347	83.33	0.1064
14.0	0.272	71.43	0.0912
16.0	0.218	62.50	0.0798
18.0	0.176	55.56	0.0709

a. Numerically equal to p/p^0.
b. For the solution of the specified concentration.
c. For the $LiCl/Ca(OH)_2$ solid mixture containing 0.1 mole of LiCl per mole of $Ca(OH)_2$.

The calculated curves for the systems $Na_2CO_3/Ca(OH)_2$ and $CaCl_2/Ca(OH)_2$ compare much less favorably with the experimental data. The comparisons are made in Figure 5-8. Two calculated curves are shown in the plot that for the Na_2CO_3 additive; one curve pertains to the above-postulated transformation to NaOH (9) and the other to the retention of Na_2CO_3 per se (9). Neither curve is an adequate representation of the data. The onset of a sharp uptake of water vapor much above the p/p^0 value expected for NaOH but below the value expected for Na_2CO_3 suggests that both sodium compounds may be present in the mixture. The curve given for $CaCl_2$ (14) is also a poor representation of the data. A possible explanation for the deviation of the results for $CaCl_2$ from those expected is the interaction of $CaCl_2$ and $Ca(OH)_2$ to produce a double salt such as $CaCl_2 \cdot Ca(OH)_2 \cdot H_2O$. Linke's solubility treatise (15) indicates that when $Ca(OH)_2$ is in stoichiometric excess over $CaCl_2$, the latter salt cannot exist as such but is transformed to the basic chloride. Thus, water-vapor attraction would be controlled by the basic chloride, not the normal chloride. Ruiz-Alsop and Rochelle (5) have reported evidence for the basic chloride as the result of x-ray diffraction studies of $CaCl_2/Ca(OH)_2$ mixtures.

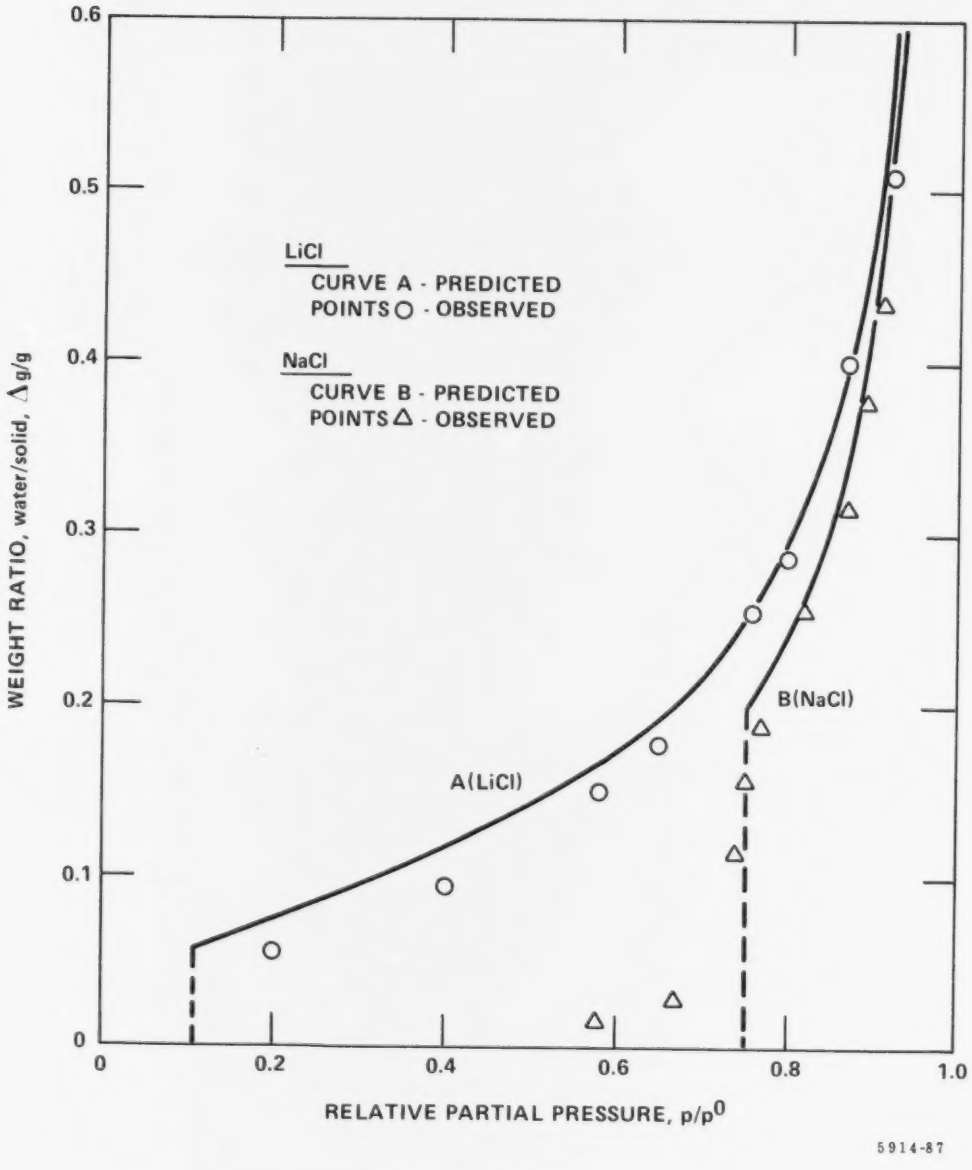

Figure 5-7. Comparison of predicted and observed adsorption relationships of $LiCl/Ca(OH)_2$ and $NaCl/Ca(OH)_2$ systems.

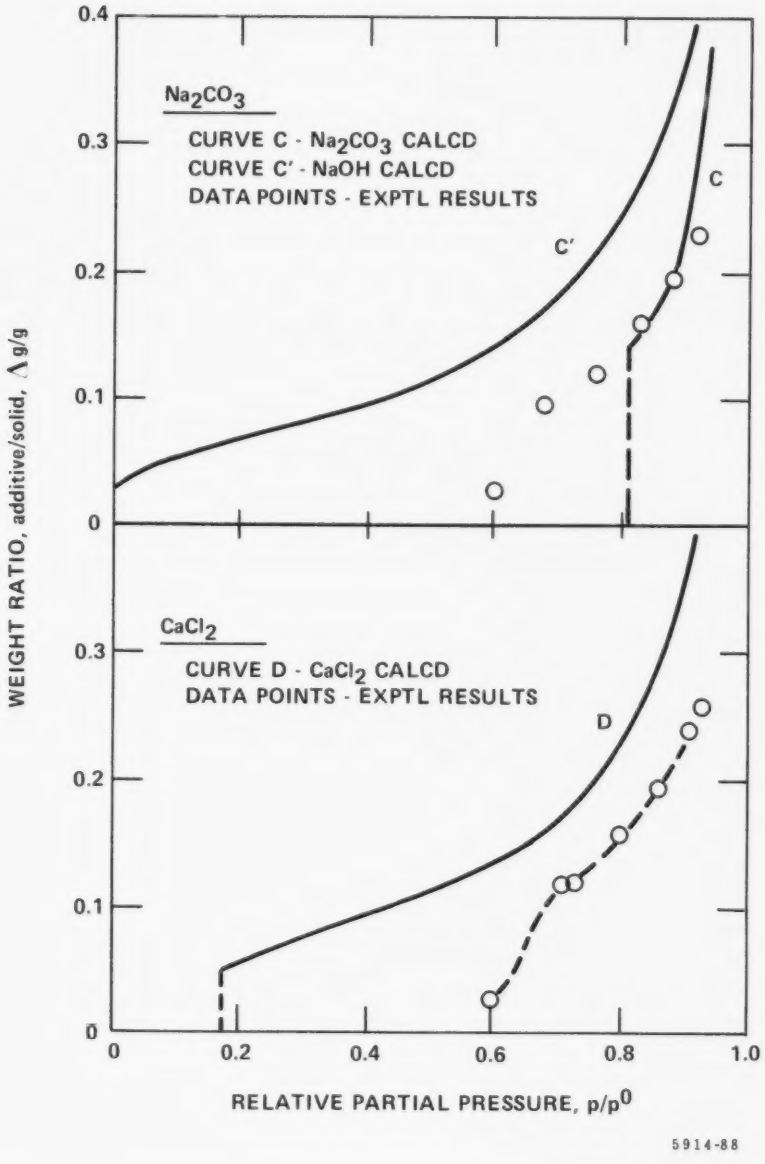

Figure 5-8. Comparison of predicted and observed adsorption relationships of $Na_2CO_3/Ca(OH)_2$ and $CaCl_2/Ca(OH)_2$ systems.

CONCLUSIONS

The ability of a water-attracting additive to influence water-vapor uptake by $Ca(OH)_2$ can sometimes be predicted, but not always. For some additives, the onset of deliquescence by the mixture with $Ca(OH)_2$ occurs near the same humidity level as when the effect occurs with the pure additive; examples of additives whose effects are predictable are LiCl and NaCl. For other additives, the effect in a mixture cannot be quantitatively predicted. An example of an additive in the later category is $CaCl_2$, which has diminished ability to attract water vapor when it combines with $Ca(OH)_2$ to form an intermediate basic chloride, $CaCl_2 \cdot Ca(OH)_2 \cdot H_2O$.

This investigation was not extended as far as originally planned, to include determinations of the effect of selected water-attracting additives on the reactivity of $Ca(OH)_2$ with SO_2 and to identify humidity ranges where enhanced reactivity occurs. The results of other investigations now available make it apparent, however, that deliquescence alone does not control the enhancement of reactivity that is provided by additives. The factors that are controlling cannot now be identified. Ruiz and Alsop (5) have suggested that additives may change the pore structure of the reaction product of $Ca(OH)_2$ and SO_2 and may make the interior may accessible to further reaction; their idea is only speculation, however, and cannot be proved right or wrong from existing information.

The above conclusion has already been made in terms of the results of Yoon et al.(6); it is made again in a somewhat different vein in Figure 5-9, which is a plot of the relationship between p/p^0 and the degree of approach to adiabatic saturation. In this figure, the relationship between p/p^0 and approach temperature is based on an assumed gas temperature of 300 °F (150 °C) and a water-vapor concentration of 7% prior to humidification with a water spray. Data points are located on the curve at p/p^0 values where deliquescence of three sodium-based additives begins. Consider NaCl as a specific example; it does not become deliquescent unless p/p^0 reaches a value of about 0.75 (about the same value regardless of temperature). To reach $p/p^0 = 0.75$ by adiabatic humidification of flue gas, the approach to saturation must be about 10 °F (5 °C). Yet, various investigators have found that NaCl is effective without this proximity to saturation; Blythe et al. (3), for example, found that 10 mol% NaCl in $Ca(OH)_2$ doubles SO_2 removal over a wide range of Ca/S mole ratios even at an approach of 25 °F (14 °C). Clearly, therefore, some phenomenon other than deliquescence must be involved.

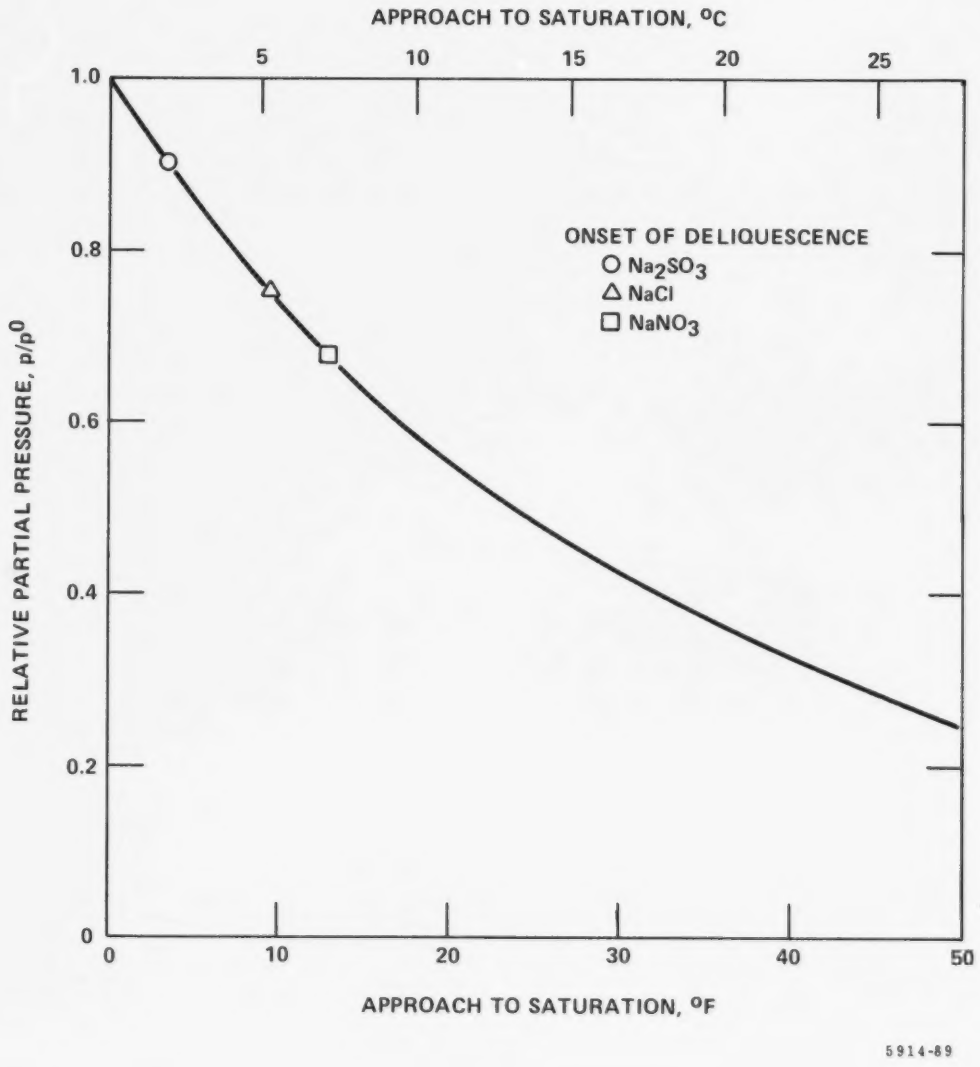

Figure 5-9. Humidities required for deliquescence versus approach to saturation.

SECTION 6

MATHEMATICAL MODELING OF HUMIDIFICATION AND SO_2 REMOVAL PROCESSES

INTRODUCTION

The process of in-duct desulfurization involves a complex set of mechanisms by which the sorbent is wetted and SO_2 is absorbed. To assist in understanding the operative mechanisms, a mathematical model was developed. This "first-generation" model treats the process in two steps. First, the "activation" of the sorbent is modeled in terms of the collisions between sorbent particles and water droplets. Second, the capture of SO_2 by the activated sorbent is modeled in terms of gas-phase diffusion of SO_2 to the sorbent/droplet ensemble, chemically enhanced absorption into the liquid phase, and liquid-phase mass transfer of the reacting species.

Based on the modeling results obtained thus far, the model appears to apply to the humidification of sorbent from either low-temperature or furnace injection. This suggests that the relatively low degree of sulfation achieved in furnace injection is not a limiting factor in the absorption of the SO_2 by the wetted sorbent. That is to say, the sulfate shell does not prevent the dissolution of a sufficient amount of lime into the droplet. This is basically a result of the very small fraction of the lime that must be dissolved in order to saturate the surrounding droplet. This will be discussed in more detail later.

SORBENT WETTING AND ACTIVATION

In the first-generation model, activation of the sorbent occurs only by physical contact between sorbent particles and water droplets. The model ignores the adsorption and transient condensation of water vapor on the sorbent particles. These mechanisms may contribute to sorbent wetting under certain circumstances. However, comparative tests with water sprays and steam humidification have shown that sorbent/droplet collision is the primary mechanism of sorbent activation (16). In any case, the model could be easily modified to accommodate the other wetting mechanisms.

Inertial impaction theory is used to model the collisions between sorbent particles and water droplets. In this treatment, the fraction of sorbent particles colliding with water droplets is a function of the relative velocity between the particles and droplets and the target efficiency for a given particle size and droplet size. The target efficiency is given by the Ranz and Wong correlation for impaction of two spheres (17). Particle size, droplet size, and relative velocity determine the target efficiency.

Since both the droplet velocity and the droplet size change during the humidification and desulfurization processes, the model must also account for the effects of droplet deceleration and droplet evaporation. The droplet leaves the nozzle at a velocity much higher than the flue gas velocity and is

rapidly decelerated by the relatively stagnant gas. This process is modeled in terms of the well-known drag relationships for spheres moving through a gas. The drag is determined by the droplet size, relative velocity, gas density, and gas viscosity. Since the gas density and viscosity depend on temperature, the model includes a heat balance to calculate the cooling of the gas due to droplet evaporation.

As expected, the drag calculations predict that the small droplets used in most previous research are rapidly decelerated. This means that they travel only a very short distance away from the nozzle before the relative velocity becomes negligible and impaction ceases. The distance of travel, and hence the degree of impaction, becomes much greater, as the droplet size is increased. For example, for droplet sizes of 20 μm and 200 μm, the "stopping" distances are about 1 in. (2.5 cm) and 6 ft (1.8 m), assuming an initial velocity of 66 ft/s (20 m/s).

The droplet evaporation rate is calculated from the mass transfer coefficient and the driving force. The latter is based on the difference between the vapor pressure at the liquid interface and the partial pressure of water vapor in the bulk flue gas. The mass transfer coefficient is based on the Froessling correlation for mass transfer from a sphere (18). This correlation relates the mass transfer coefficient to the droplet size, relative velocity, gas density, gas viscosity, and the diffusivity of water vapor. The droplet evaporation rate predicted using this correlation is used to calculate the change in droplet size and simultaneously update the water vapor concentration in the flue gas.

Droplet evaporation and deceleration begin simultaneously as soon as the droplet leaves the nozzle and enters the flue gas stream. Thus, the droplet is shrinking while it is decelerating. For practical droplet sizes, however, the stopping distance is so short that the shrinkage during deceleration is negligible. Under these conditions, a plot of the stopping distance versus the droplet size should show the same trend as terminal velocity versus droplet size. Thus, an internal check on the model calculations is provided by comparing the size-dependence of these parameters. In this manner, the calculations have been confirmed over a range of conditions.

In order to accurately simulate various commercial lime sorbents and water spray nozzles, the model must take account of the particle and droplet size distributions. Thus, the model must integrate the inertial impaction calculations over the entire range of sorbent particle size and droplet size, taking into account the two size distributions. This is accomplished by first integrating over the particle size distribution to obtain the overall fraction of particles wetted by each droplet size. This result is then integrated over the droplet size distribution to obtain the overall fraction of sorbent wetted by all droplets. This fraction of the sorbent is assumed to be activated for SO_2 capture.

SO_2 CAPTURE

Calculations of SO_2 capture are applied to only the wetted fraction of sorbent particles. It is assumed that the sorbent/droplet ensembles can be

treated in a manner analogous to the slurry droplets produced in a spray dryer. Therefore, this process is treated by a modified version of an existing spray dryer model. The basics of this model will not be discussed here, since they have been described in detail elsewhere (19). The original model was based on a mean slurry droplet size. However, our modeling work has shown that treatment of only the mean size can result in significant error compared to use of the actual size distribution (6, 20). Therefore, the spray dryer model was modified to accommodate the size distribution of sorbent/-droplet ensembles predicted by the inertial impaction treatment.

The original spray dryer model also included the approximation that the Sherwood number remained constant at a value of 2. This assumption is valid only when the relative velocity becomes vanishingly small, which is not the case during droplet deceleration. Therefore, this assumption was replaced by a rigorous calculation of the Sherwood number based on a Froessling correlation analogous to that used in the droplet evaporation calculations. This modification can have a major impact on the results when the time required for droplet deceleration represents a significant portion of the total residence time.

Under typical spray dryer conditions, the chemical reaction between the dissolved lime and SO_2 provides a significant enhancement over purely physical absorption. Damle (19) has shown that this enhancement increases the liquid-phase mass transfer by a factor of 200 for a 50-μm slurry droplet at 120 °F (50 °C). Therefore, the rate-limiting mechanism is usually either the gas-phase diffusion of SO_2 to the droplet or the rate of lime dissolution.

When gas-phase diffusion is controlling, the spray dryer model should be directly applicable to the case of reactivating sorbent from furnace injection. However, the applicability of the model may be questioned when lime dissolution is controlling, since the sulfate shell on the sorbent may retard the dissolution rate. This effect may be examined by calculating the fraction of the sorbent that must be dissolved in order to saturate a droplet of given size.

For the mean sorbent and droplet sizes of 3.5 μm and 20 μm, complete dissolution of the sorbent would result in a lime concentration of 0.316 moles/L in the droplet. At 130 °F (55 °C), the solubility of lime in water is 0.016 moles/L (21). Thus, only about 5% of the sorbent must be dissolved in order to saturate the droplet. Since furnace injection generally results in less than 30% sorbent utilization, it appears likely that 5% of the sorbent could be available for dissolution. Therefore, the partial sulfation of the furnace injected sorbent does not necessarily preclude the possibility that a sufficient amount of lime can be dissolved. The dissolution of lime from the spent sorbent is also suggested by the rapid increase in pH when a spent sorbent is slaked (22).

Partially sulfated sorbent also releases heat when it is wetted due to the exothermic hydration of the lime. The practical effect on droplet temperature is minimal, however, since the relatively large water droplet acts as an infinite heat sink for the much smaller lime particle. For the case of typi-

cal mean particle and droplet sizes, the mass ratio is over 300. Based on a heat of hydration (23) of 490 Btu/lb (270 cal/g), the maximum droplet temperature rise would be 1.6 °F (0.9 °C). The effect of this small temperature rise is negligible.

LIMITING ASSUMPTIONS

For the impaction calculations, it is assumed that the sorbent particles and the water droplets are evenly distributed across the duct at the plane where impaction begins. This case may be approached when the sorbent is injected well upstream to allow good dispersion and the water is sprayed through a large array of nozzles. If the sorbent is stratified or the nozzles do not provide uniform coverage, the model will over-predict the degree of wetting.

The drag calculations assume that the droplets are immediately subject to the drag of the surrounding gas. This assumption is valid for a single-fluid nozzle where the injected droplets are immediately enveloped in flue gas. With two-fluid nozzles, however, the carrier air would insulate the droplets from the drag. The high-velocity carrier air would also create a low-pressure zone that would entrain sorbent particles into the jet. Calculations have shown that the net effect of the insulation and entrainment is a reduction in sorbent/droplet contacting (21). Thus, the model will tend to over-predict the degree of wetting achieved with two-fluid nozzles. However, there is no such limitation for single-fluid nozzles.

In the region near the water spray nozzle, where there is maximum droplet deceleration and maximum sorbent/droplet collision, the flow is assumed to be one-dimensional and incompressible. That is, the sorbent particles and water droplets travel along the axis of the spray nozzle, and impaction occurs when a droplet overtakes a sorbent particle. In reality, the spray trajectory is at an angle to the gas flow, which the fine sorbent particles tend to follow closely. This angle is greatest near the nozzle, where the droplet velocities are highest. In this region, the sorbent particles are effectively stagnant, so the relative velocity is independent of trajectory. Thus, the impaction calculations are still valid even though the streamlines are not co-directional.

MODELING RESULTS

The mathematical model has been used to examine the dependence of predicted SO_2 capture on the approach to saturation (or amount of water injected), Ca/S ratio, residence time, and droplet size. The predicted effects of these parameters are illustrated in Figures 6-1, 6-2, and 6-3. These effects apply equally to the injection of hydrated lime at low temperature or reactivation of furnace-injected sorbent.

Figure 6-1 shows the effect of approach to saturation and Ca/S ratio. These predictions are based on an assumed flue gas velocity of 50 ft/s (15 m/s), residence time of 2 s, inlet flue gas temperature of 300 °F (150 °C), and inlet flue gas moisture content of 8% by volume. These parameters are believed to be reasonably representative of many pre-NSPS boiler

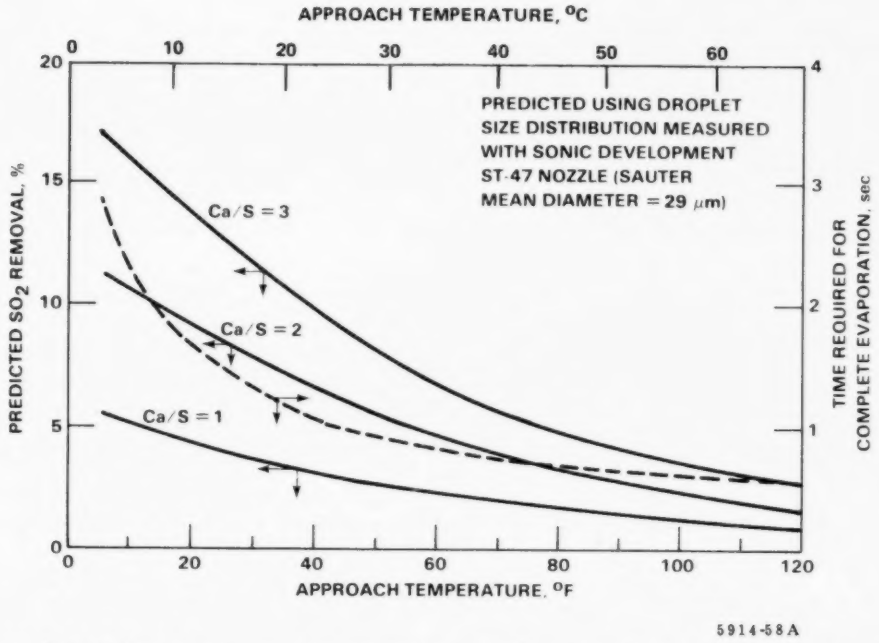

Figure 6-1. Effect of approach to saturation on SO_2 removal and evaporation time.

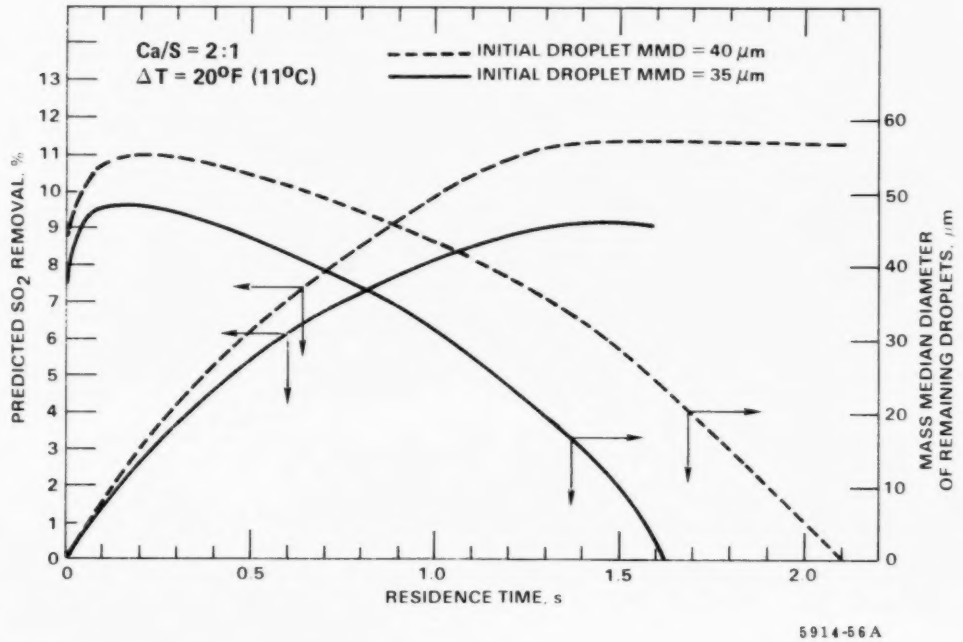

Figure 6-2. Predicted SO_2 removal and droplet MMD as a function of residence time.

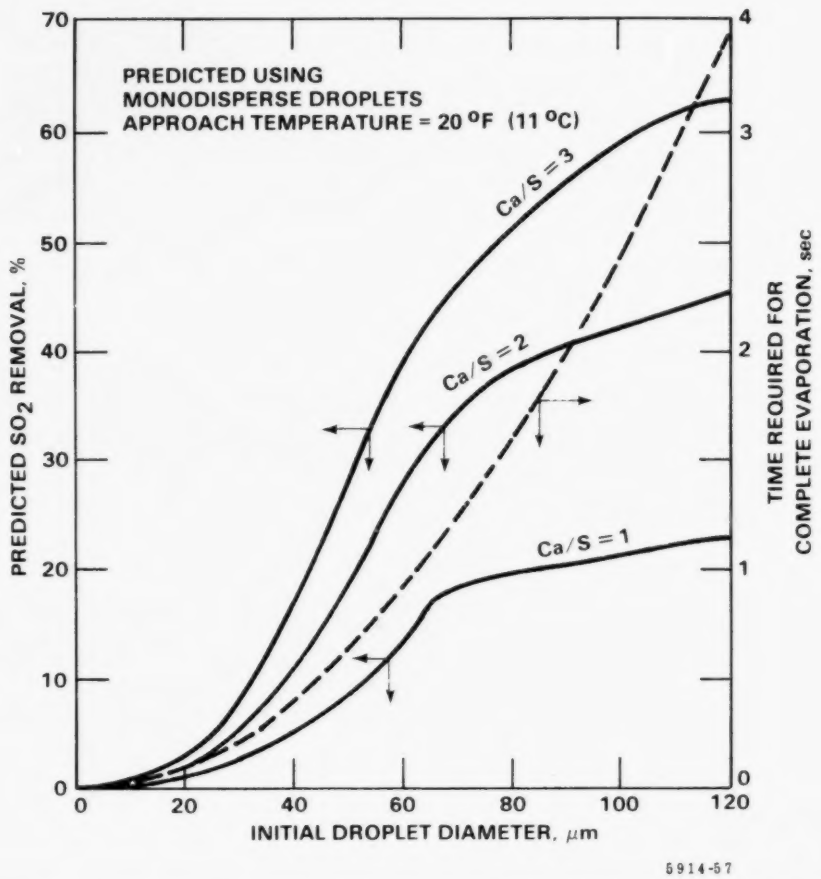

Figure 6-3. Effect of initial drop diameter on SO_2 removal and evaporation time.

retrofits. An initial droplet velocity of 460 ft/s (140 m/s) was chosen based on data supplied by Sonic Development Corporation for their ST-47 nozzle, which was the nozzle used in most of Southern Research's tests. The initial droplet size distribution was based on measurements made with a video droplet analyzer (24) under cold-flow conditions. The Sauter mean and mass mean diameters were 29 μm and 24 μm, respectively. The minimum and maximum sizes were 15 and 71 μm, respectively.

All of the modeling was done using a sorbent particle size distribution obtained from cascade impactor measurements made in the Southern Research pilot combustor while firing coal and injecting hydrated lime. The sorbent size distribution was obtained by subtracting the fly ash distribution from the ash/sorbent distribution. The resulting sorbent distribution had a mass median diameter (mmd) of about 4 μm. This is comparable to the mmd of fresh hydrated lime sized by sedimentation in a dispersant liquid. This suggests that the high-temperature injection process results in very good dispersion of the hydrated lime. This degree of dispersion may not be attainable at low temperatures due to agglomeration. The effect of varying degrees of sorbent

dispersion could be examined by using different sorbent size distributions in the model. This has not yet been done.

The effect of residence time on the predicted SO_2 capture is illustrated in Figure 6-2. This figure also illustrates how the mean droplet size changes with residence time. The figure shows that SO_2 removal ceases when the droplets are totally evaporated; this prediction, however, is a limitation of the present model, since even the residual dry solid will react at a finite rate. These predictions were based on a Ca/S ratio of 2:1 and an approach temperature of 20 °F (11 °C). The values of all other parameters were the same as those given previously.

Figure 6-3 shows the predicted effect of initial droplet size on the SO_2 capture and the time required for complete evaporation. While larger droplets give better removal, they also require more time to evaporate. For most retrofits, the available residence time would be less than 3 s. For the conditions studied, this would limit the maximum droplet size to 110 μm. These predictions are based on an approach temperature of 20 °F (11 °C) and Ca/S ratios of 1:1, 2:1, and 3:1, with all other independent variables held constant at the values given above.

The model predicts that there is an optimum droplet size with respect to SO_2 capture. This optimum corresponds to the maximum degree of sorbent wetting, or maximum sorbent/droplet collision rate. An optimum size exists due to the trade-off between increasing stopping distance and decreasing coverage of the duct cross section. Larger droplets are able to penetrate further into the flue gas and impact more sorbent particles. However, for a fixed flowrate of water (or fixed approach to saturation), larger droplets give less coverage of the duct cross section. This results is an optimum droplet size, which is typically about 150 to 200 μm for the conditions studied. Unfortunately, such a large droplet size is impractical due to the required evaporation time and problems with wall wetting. However, if a system could be designed to tolerate wall wetting and incomplete evaporation, much higher SO_2 removals could be achieved.

CONCLUSIONS

When lime and water are injected separately, the SO_2 removal efficiency is governed by the degree of sorbent wetting by collisions between sorbent particles and water droplets. The sorbent/droplet collision rate is maximized by making the droplet size and velocity as large as possible. In actual practice, however, the droplet size must be well below the optimum value in order to ensure complete evaporation and avoid wetting of the duct walls. If the humidification process could be modified to allow larger droplets, it would be possible to significantly improve on the sulfur capture achieved.

In addition to droplet size and velocity, the sulfur capture is strongly influenced by approach to saturation, Ca/S ratio, and residence time. To maximize SO_2 removal, the approach should be as close as possible. However, it may be difficult to consistently maintain dry duct walls at approaches of less than 20 °F (11 °C). Increasing the sorbent injection rate, or Ca/S ratio, is also beneficial, but reaches a point of diminishing returns due to

increased operating cost and particulate loadings. The effect of the latter on ESP performance must also be considered.

Increasing the residence time is only beneficial up to the point of complete droplet evaporation. Conversely, the residence time must be at least sufficient to allow complete evaporation. For most retrofit situations, the residence time will be fixed. This means that the droplet size must be selected to make maximum use of the available time without allowing droplets to reach the ESP. The model can be used to predict the optimum droplet sizing for a given duct residence time.

Strictly speaking, this mathematical model applies only to single-fluid nozzles, since each injected droplet is assumed to be immediately surrounded by the flue gas. That is to say, the entrainment and insulation associated with a two-fluid jet are not modeled. The net effect of these mechanisms is to reduce the sorbent/droplet collision rate compared to the single-fluid case. Therefore, the model predicts an upper limit on SO_2 removal achieved with two-fluid nozzles.

The modeling results strongly suggest that larger droplet sizes should be used to improve SO_2 removal. This improvement must be weighed against the longer residence time required for droplet evaporation. The potential for wall wetting must also be given consideration. Even with these considerations, it appears to be practical to use droplets larger than those produced by the Sonic Development ST-47 nozzle (Sauter mean = 29 μm). Sauter mean sizes on the order of 40 to 60 μm should be evaluated in future tests.

The effect of sorbent particle size also needs to be investigated further. It may be possible to enhance the rate of sorbent/droplet collisions by increasing the sorbent particle size through agglomeration. This may offer an alternative to the use of coarser water sprays as a means of increasing collision frequency.

SECTION 7

REFERENCES

1. Yoon, H., M.R. Stouffer, W.A. Rosenhoover, and R.M. Statnick. Laboratory and Field Development of Coolside Abatement Technology. Second Annual Pittsburgh Coal Conference, Pittsburgh, PA. September 1985.

2. Jorgensen, C., J.C.S. Chang, and T.G. Brna. Evaluation of Sorbents and Additives for Dry SO_2 Removal. Environ. Progress 6(2): 26, February 1987.

3. Blythe, G., R. Smith, M. McElroy, R. Rhudy, V. Bland, and C. Martin. EPRI Pilot Testing of SO_2 Removal by Calcium Injection Upstream of a Particulate Control Device. In: Proceedings: 1986 Joint Symposium on Dry SO_2 and Simultaneous SO_2/NO_x Control Technologies, Volume 2. EPA-600/9-86-029b (NTIS PB87-120457). U.S. Environmental Protection Agency, Research Triangle Park, NC. October 1986. p. 35-1.

4. Karlsson, H.T., J. Klingspor, M. Linné, and I. Bjerle. Activated Wet-Dry Scrubbing of SO_2. J. Air Pollut. Control Assoc. 33: 23, 1983.

5. Ruiz-Alsop, R.N., and G.T. Rochelle. Effect of Deliquescent Salt Additives on the Reaction of SO_2 with $Ca(OH)_2$. American Chemical Society National Meeting, Miami, FL. April 1985.

6. Yoon, H., J.A. Withum, W.A. Rosenhoover, and F.P. Burke. Sorbent Improvement and Computer Modeling Studies for Coolside Desulfurization. In: Proceedings: 1986 Joint Symposium on Dry SO_2 and Simultaneous SO_2/NO_x Control Technologies, Volume 2. EPA-600/9-86-029b (NTIS PB87-120457). U.S. Environmental Protection Agency, Research Triangle Park, NC. October 1986. p. 33-1.

7. Gibbard, H.F., Jr., G. Scatchard, R.A. Rousseau, and J.L. Creek. Liquid-Vapor Equilibrium of Aqueous Sodium Chloride, from 298 to 373K and from 1 to 6 mol kg^{-1}, and Related Properties. J. Chem. Eng. Data 19: 281, 1974.

8. Carr, D.S., and B.L. Harris. Solutions for Maintaining Constant Relative Humidity. Ind. Eng. Chem. 41: 2014, 1949.

9. Washburn, E.W. (editor). International Critical Tables of Numerical Data, Physics, Chemistry, and Technology, Volume III. McGraw-Hill Book Company, New York, NY. 1928. pp. 361-374.

10. Goldberg, R.N. Evaluated Activity Osmotic Coefficients for Aqueous Solutions: Thirty-Six Uni-Bivalant Electrolytes. J. Phys. Chem. Ref. Data 10: 671, 1981.

11. Gibbard, H.F., Jr., and G. Scatchard. Liquid-Vapor Equilibrium of Aqueous Lithium Chloride, from 25 to 100 °C and from 1.0 to 18.5 Molal, and Related Properties. J. Chem. Eng. Data 18: 293, 1973.

12. Glasson, D.R. Reactivity of Lime and Related Oxides. II. Sorption of Water Vapor on Calcium Oxide. J. Appl. Chem. 8: 798, 1958.

13. Klingspor, J., A. Strömberg, H.T. Karlsson, and I. Bjerle. Similarities between Lime and Limestone in Wet-Dry Scrubbing. Chem. Eng. Process. 18: 239, 1984.

14. Harrison, W.R., and E.P. Perman. Vapor Pressure and Heat of Dilution of Aqueous Solutions. Trans. Faraday Soc. 23: 1, 1927.

15. Linke, W.F. Solubilities of Inorganic and Organic Compounds. D. Van Nostrand, Princeton, NJ. Fourth Edition. 1958. p. 634.

16. Yoon, H., M.R. Stouffer, and F.P. Burke. Coolside Desulfurization Reactions and Mechanisms. National Meeting of the American Chemical Society, New Orleans, LA. August-September 1987.

17. Ranz, W.E., and J.B. Wong. Impaction of Dust and Smoke Particles, Ind. Eng. Chem. 44: 1371, 1952.

18. Froessling, N. The Evaporation of Falling Drops. Gerlands Beits. Geophys. 52: 170, 1938.

19. Damle, A.S. Modeling of SO_2 Removal in Spray-Dryer Flue-Gas Desulfurization System. EPA-600/7-85-038 (NTIS PB86-136165). U.S. Environmental Protection Agency, Research Triangle Park, NC. December 1985.

20. Stokes, E.A. Southern Research Institute, Birmingham, AL. Personal Communication to D.C. Drehmel, March 2, 1987.

21. Josewicz, W., and G. Rochelle. Modeling of SO_2 Removal by Spray Dryers. Pittsburgh Coal Technology Conference, Pittsburgh, PA. September 1984.

22. Dahlin, R.S., C.L. Lishawa, and N. Kaplan. Analysis of LIMB Waste Management Options. In: Proceedings: 1986 Joint Symposium on Dry SO_2 and Simultaneous SO_2/NO_x Control Technologies, Volume 2. EPA-600/9-86-029b (NTIS PB87-120457). U.S. Environmental Protection Agency, Research Triangle Park, NC. October 1986. p. 39-1.

23. Boynton, R.S. Chemistry and Technology of Lime and Limestone. Wiley-Interscience, New York, NY. Second Edition. 1980. p. 324.

24. Muzio, L.J. Fossil Energy Research Corporation, Laguna Hills, CA. Personal Communication to J.P. Gooch, December 11, 1986.

APPENDIX

QUALITY CONTROL EVALUATION REPORT

Quality Assurance Project Plan (QAPP)

The work described in this topical report was supported through Cooperative Agreements CR 811683 and CR 812811. The experimental measurements described here were guided by the Quality Assurance Project Plan submitted under CR 811683 on June 1, 1985. This QAPP was approved by EPA in January 1986. The QA procedures in this QAPP were adopted for CR 812811 because of the similarity of the experimental objectives and requirements.

All experimental tasks were designated by EPA as QA Category III. Tasks in this category support technology development programs in the Air and Energy Engineering Research Laboratory or in one of the Divisions or Branches, with the possibility of leading to further work in support of broader technical objectives.

Management and Technical Systems Audits

On July 15, 1985, EPA conducted a Management Systems Audit (MSA) and a Technical Systems Audit (TSA) on CR 811683. Based on the results of these audits, the program was rated as "Acceptable, with Qualifications". The major qualifications were that separate QAPPS be prepared for two of the five project tasks and that Standard Operating Procedures (SOPs) be more thoroughly documented for certain measurement systems. Southern Research responded by upgrading existing SOPs, writing some new SOPs, and by preparing and submitting separate QAPPs as required. Since the measurement efforts described in this topical report are covered under the original basic QA plan, the separate QA plans for the other tasks are not relevant.

Evaluation of Measurement and Analytical Systems

All measurement and analytical systems were operated in accordance with the procedures given in the QAPPs. Accuracy was checked using NBS Standard Reference Materials (SRMs) and additional primary standards when appropriate. Precision was checked by use of duplicate runs and sample replicates. In general, the precision and accuracy of each system was found to be within the data quality objectives specified in the appropriate QAPP. For example, the precision and accuracy of the SO_2 measurements, which represent one of the most critical data elements in the project, were 6% and 3.6%, respectively. These are well within the objectives of 10% and 5%. Multipoint calibrations revealed excellent linearity in the instrument response. The critical measurements which relate to this topical report are discussed below.

Coal and sorbent feed rates. Coal and sorbent feed rates to the Southern Research pilot combustor were checked by weighing the amount of material discharged during a fixed time interval. The actual coal feed rate was found to be typically within 1% of the set point on the gravimetric feeder. Sorbent feed rates were slightly less dependable due to the smaller amount of material being fed.

Air and water flow rates. The flow rate of combustion air was monitored with orifice meters, and the flow rate of sorbent transport air was monitored with a rotameter. Both measurements were corrected for actual line temperature and pressure. Although the flow meters in each case are used to set up test conditions, these flow rates are not normally used in any calculations like those in the present work. The flue gas rate is required for calculation of sorbent stoichiometry (in conjunction with the SO_2 concentration). The flue gas rate is based on the coal feed rate, coal composition, and flue gas oxygen content; combustion air flow rate is not required.

The flow of water used for humidification of the flue gas was measured with a Matheson rotameter. The rotameter was calibrated by weighing timed discharges at several different flow rates over the range of the instrument. As with the air flow rates, the water flow rate was used only to check the consistency of the primary variables of interest. In the case of humidification, these variables are the approach to saturation and the absolute temperature.

Chemical analysis of ash and sorbent samples. All chemical analyses of ash and sorbent samples were checked for accuracy by the use of NBS SRM fly ash (SRM No. 1633a) and limestone (SRM No. 1c). Accuracies on all elements were well within the data quality objectives. Precisions were checked by replicate analyses of an Eastern U.S. fly ash. All relative standard deviations (RSDs) were under 2.5% except for SO_3, which had an RSD of 12%. This exceeded the data quality objective of 9%, which was based on past experience. This difference was not considered to be critical since sorbent utilization is based on soluble sulfate rather than sulfur trioxide.

Analysis of flue gas. A stream of flue gas was drawn through an in-stack, porous stainless steel filter. The gas was then drawn through a dehumidifier, which reduced the dewpoint to the range 32-40 °F (18-22 °C), and next through a second in-line filter, which ensured virtually complete removal of suspended fly ash. The gas was then distributed through switching values to the individual analyzers:

Beckman Model 755 Paramagnetic, O_2

Beckman Model 864 Nondispersive Infrared, CO_2

DuPont Model 400 Ultraviolet, SO_2

ThermoElectron Model 10 Chemiluminescent, NO_x

Horiba Model PIR-2000 NDIR, CO

All instruments were kept in dependable service on the basis of regular calibrations with certified calibration gases.

Since the SO_2 content of the flue gas was a major focus in this work, additional quality assurance procedures were carried out for the DuPont Model 400 analyzer. These included multipoint calibrations, use of NBS Standard Reference Materials (SRMs), and the keeping of detailed records of instrument calibration and performance.

Daily calibration of the SO_2 analyzer was performed using a single, Matheson Primary Standard grade gas. A log of instrument response and dial settings before and after calibration was kept using the Daily Calibration Record.

Precision and accuracy of the SO_2 analyzer may be estimated from a record of the instrument response to span gas taken during the daily calibration before adjustment to the span value. Forty-one such values recorded over a six-month period yielded the following:

span gas concentration	1997
average of 41 values	2011
standard deviation, ppm	120
standard deviation, %	6.0
average of $\left\lvert\frac{Xi-1997}{1997}\right\rvert$*100	3.6

The values 6.0 and 3.6% represent the precision and accuracy, and are well within the respective goals of 10 and 5% for this measurement. Note that the record used to arrive at the foregoing accuracy and precision included readings taken after 2-day to 2-week down periods, whereas calibration always preceded actual tests by less than 24 hours.

Multipoint calibrations were performed periodically to determine instrument linearity and to verify the concentration of the single calibration gas used for daily adjustments. Figure A-1 shows an example of this technique. The instrument was first calibrated using the Daily Calibration procedure with 1997 ppm Matheson Primary Standard gas. Then, without further adjustment to the instrument, three NB$ Standard Reference Materials and an additional Primary Standard gas were sampled. Linearity was excellent, and the absolute values of the SRM materials were within the tolerances given by NBS.

Determination of sorbent utilization. This was the primary task in the combustor experimentation. Usually, the extent of utilization was based on two factors: (1) the mole ratio of sorbent to SO_2 and (2) the percentage reduction in SO_2:

$$\text{Utilization, \%} = \frac{\Delta[SO_2),\ \%}{Ca/S}$$

Precautions were taken to ensure that the observed change in SO_2 concentration was due to the change in conditions under consideration, not to due to some secondary factor. Recorder traces showing SO_2 concentration versus time were used to differentiate changes occurring as the result of reaction with sorbent in the suspended state and reaction with sorbent deposited on walls of the reaction system. Generally speaking, only the effect occurring in the suspended state was relevant to the issue being investigated. Illustrations of time-dependent changes in SO_2 concentration are given in Figures 3-3, 3-4, 3-5, 4-4, and 4-11 of this report.

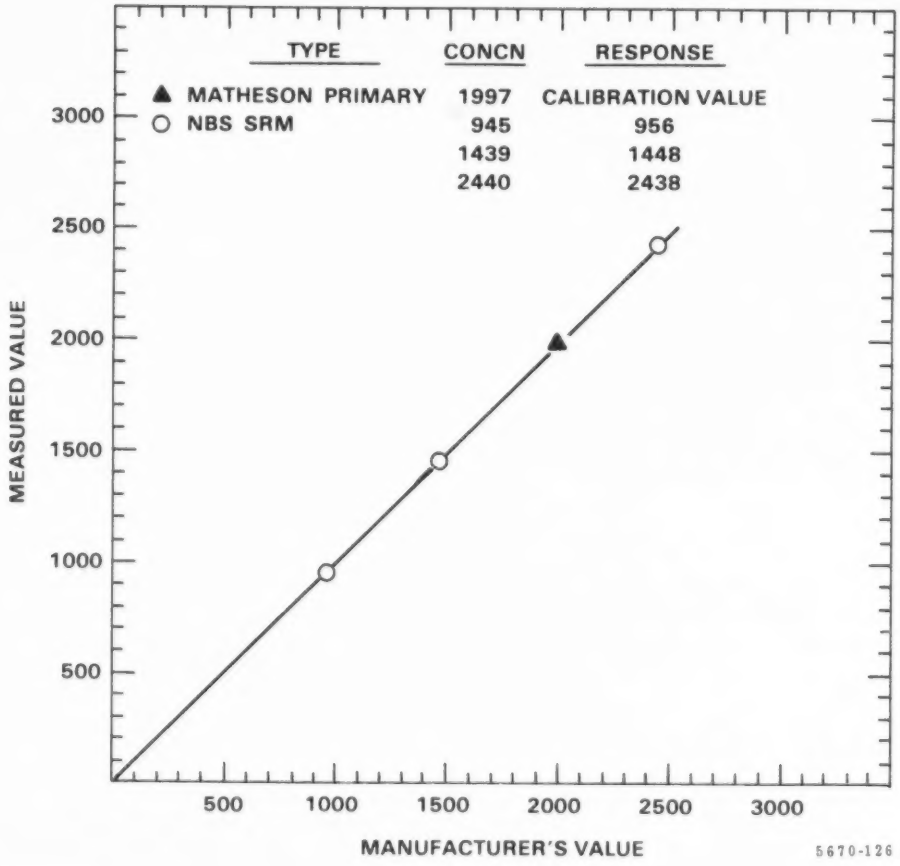

Figure A-1. Multipoint calibration of Dupont SO_2 Analyzer.

On occasion, determinations of SO_2 concentration alone could not be depended upon for calculation of utilization. Then, extraction of solids from the gas stream and analysis of the sulfate-to-calcium ratio in the spent sorbent were required for determination of utilization:

$$\text{Utilization, \%} = \frac{\text{moles sulfate}}{\text{moles calcium}} \times 100$$

The design and validation of an extraction probe for entrained solids are discussed in Section 3 of this report.

Auxiliary sampling equipment. Calibration of auxiliary sampling equipment included checking dry and wet test meters, checking tolerances on sampling nozzles, checking resistivity probe electrode spacing with calipers, checking tolerances on cascade impactor hole sizes and jet to plate spacings, calibrating impactors with known aerosols, and calibrating the electrobalance used to weigh the particulate catches.

Sample Custody and Tracking

Sample custody and tracking requirements were met as specified in the QAPP. All samples were assigned unique Southern Research notebook numbers referring to the page and section in which they are described in the laboratory notebook. Sample containers were marked with the corresponding numbers and other appropriate identifying information.

Internal Audits, QC Checks, and Corrective Measures

An internal audit by the Southern Research QA Manager revealed no serious deficiencies in the internal QC checks and data reduction. However, recommendations were made to standardize the use of laboratory notebooks for recording data during field measurement activities. This replaced the use of loose-leaf binders and loose forms. In cases where the forms were desirable, they were attached in the notebook. This facilitated access to the data for subsequent QC checks.

Limitations of Use of Data

The most significant limitation on the use of these data is that they should not be applied outside the range of the conditions studied. For example, the SO_2 removal data should not be used to predict the performance of a full-scale LIMB retrofit unless the boiler temperature profile and injection conditions are known to be similar to those given here. In particular, the extent of removal of SO_2 effected by a humidification system in a full-scale plant will be determined in part by reaction with entrained solids and in part by reaction with deposited solids. The data from this research are expected to predict the extent of the suspended-phase reaction alone.